



PhD Course in Biomedical Sciences and Biotechnology

33rd Cycle

Year 2020-21

GLUTARALDEHYDE BASED IN-VIVO SNAP-CROSSLINKING AMENABLE TO BIOCONDENSATE SEPARATION FOR COMPOSITIONAL IDENTITY BASED ANALYSIS

PhD Candidate

Anitha Rajendran

Supervisor

Prof. Claudio Schneider

Co-supervisor

Dr. Roberto Verardo

TABLE OF CONTENTS

ABSTRACT	3
AIM OF THE THESIS	4
INTRODUCTION	5
DISORDERED PROTEINS AND LLPS	6
ROLE OF RNA IN LLPS.....	7
CAPTURING RNP COMPLEXES FOR CHARACTERIZATION.....	10
UV CROSSLINKING	10
CHEMICAL CROSSLINKING	11
GLUTARALDEHYDE	13
DIFFERENCE BETWEEN FA AND GA	14
QUENCHING	15
RESULTS	17
HIGH THROUGHPUT IMAGING TO IDENTIFY THE BEST CROSSLINKING CONDITIONS.....	18
FRAP- A REAL TIME ANALYSIS TO DETERMINE THE RESULTANT MOBILITY OF THE GFP-G3BP1 CROSSLINKED-COMPLEXES.....	20
BIOCHEMICAL ANALYSIS TO VALIDATE THE FIXATIVE CROSSLINKING CONDITIONS AS DETERMINED BY SDS-PAGE OF GFP-G3BP1 HIGH-MOLECULAR WEIGHT COMPLEXES.....	22
YAP1 AS CYTOSOL-NUCLEAR PROTEIN.....	24
P53, A NUCLEAR-TF, AS A FURTHER VALIDATION OF SNAP-SHOT CROSSLINKING.....	24
GFP-FUS AS MODEL SYSTEM TO ANALYZE SNAP-SHOT FIXATION / CROSS-LINKING EFFICIENCY OF A NUCLEAR-MARKER	25
FRAP ANALYSIS ON CROSSLINKING OF NUCLEAR FUS	26
BIOCHEMICAL EXTRACTION & SOLUBILIZATION FOR NUCLEAR LOCALIZED PROTEINS.....	28
BIOCHEMICAL FRACTIONATION OF CROSSLINKED COMPLEXES.....	29
A UNIFIED PROTOCOL FOR CYTOSOLIC AND NUCLEAR CROSSLINKED-COMPLEXES BY MAGNETIC BEADS IMMOBILIZATION AND TREATMENT FOR DIFFERENTIAL DISSOLUTION	31
PRIMARY SCREENING OF FIXATIVES FOR OPTIMIZING SHORT FIXATION PROTOCOL.....	36
DISCUSSIONS	39
MATERIAL & METHODS	44
CELL CULTURE AND MAINTENANCE	45
FIXATION	45
HIGH THROUGHPUT IMAGING	45
FLUORESCENT RECOVERY AFTER PHOTBLEACHING (FRAP).....	46
CELL DISRUPTION WITH SONICATION.....	46
SDS-PAGE AND WESTERN BLOT.....	47
IMMUNOPRECIPITATION.....	47
EXTRACTION OF COMPLEXES WITH COOH BEADS	48
REFERENCES	49
ACKNOWLEDGEMENTS.....	49

ABSTRACT

Membrane-bound organelles organize their molecular events by regulated transport of molecules through their transmembrane channels. On the other hand, Membrane-less Organelles (MLOs) are non-stoichiometric assemblies of locally concentrated molecules mainly proteins, RNAs and DNAs. MLOs are condensed liquid-like structures that appear distinct from their milieu. These condensates are highly dynamic and quickly exchange their components with their surrounding environment, resulting in a vast number of transient interactions. There is a necessary requirement to follow such dynamic compositional identity, using proteins as handles for their isolation, and to develop technologies that allow for fast in-vivo crosslinking methodologies to maintain and capture the complete picture of RNA-protein interactions as required for reconstructing the high temporal exchange dynamics. In this context, UV-crosslinking based CLIP technologies is limited in its applicability to proteins that are in direct contact with RNA (i.e., RBPs) being ill-suited to study proteins that interact with RNA indirectly within condensates. Here we have compared aldehyde-based fixatives for their ability to fix or immobilize condensate-forming GFP-tagged proteins within a one-minute snap-fixation. As a model system we have used cells constitutively expressing GFP-G3BP1 as a marker of SGs and GFP-FUS as a marker of PSs. By combining high-throughput imaging and Fluorescence Recovery After Photobleaching (FRAP) analysis we show that proper concentrations of Glutaraldehyde (GA) alone or in combination with Formaldehyde (FA) allow efficient fixation/immobilization of the respective markers within short-time interval from contacting the fixative. We then used the selected conditions to show that the protein-markers become efficiently cross-linked as assessed by western-blotting in order to further enrich by antibody-immunoprecipitation.

Keywords: phase separation, RNA-protein interactions, stress granules, crosslinking, FRAP, G3BP1, FUS, YAP, p53,

AIM OF THE THESIS

RNA-protein condensates or RNPs are dynamic structures formed by liquid-liquid phase separation (LLPS) constituting the “liquid information flow” to organize and regulate key biological processes, from chromosome condensation, transcription, splicing, and translation, to synaptic activity or receptor activation. Numerous transient interactions allow these structures to attain chemical equilibrium with their surrounding milieu. Despite vast developments in the field of cellular LLPS to identify and characterize the proteins and RNAs involved, limitations pertaining to characterizing short lived interactions still persist. The aim of our work was to find the fastest and most efficient crosslinking linking fixative to snap-shot immobilizing the RNA-protein interactions relevant to the formations RNP condensates, optimizing the conditions suitable for extraction of crosslinked complexes while maintaining their global composition. We aimed at developing a non-mechanical treatment-based method of extraction in order to avoid loss of complexes due to crosslinking for efficient immunoprecipitation of the obtained complexes for the analysis of RNA-compositional identities in selected RNP-condensates.

INTRODUCTION

The fundamental and unifying problem of the 3-Domains of Life is how the highly crowded 3D cellular space becomes organized to perform the most efficient control on complex biochemical reactions in 4D that is in space and time (Cohan and Pappu, 2020). The gain in efficiency requires that all chemical reactions must be organized within compartments to promote coordinated flow of biological matter, be it small-molecules or larger-assemblages. Therefore, the only way to coordinate and regulate in space and time, such biochemical reactions is to locate and concentrate both machinery (enzymes for metabolic-reactions) and substrates (small-molecules for metabolic-reactions) within the same compartment. This organization increases the kinetics of the reaction and limit free diffusion of both substrate and products (Weiss, 2014). If the subsequent machinery in the coordinated pathway is located in the same ‘compartment’ then the product of the first reaction is similarly more concentrated. In converse, when such ‘compartment’ is dissociated or disassembled, such coordinated and vectorial reactions lose their efficient kinetics thus becoming arrested or inhibited. In noncommittal sense, The term compartment refers to physical spaces bounded by ‘hindrances to free diffusion’; it is any restriction or confinement that limits free or passive diffusion thus allowing ‘vectoriality’ that is ‘order’ (de Lorenzo, Sekowska and Danchin, 2015).

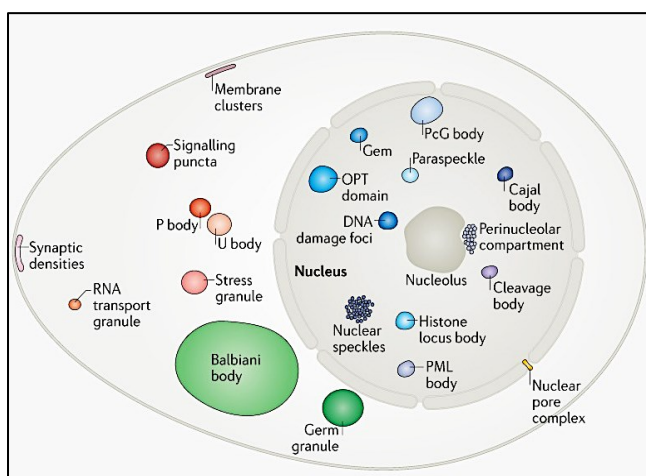
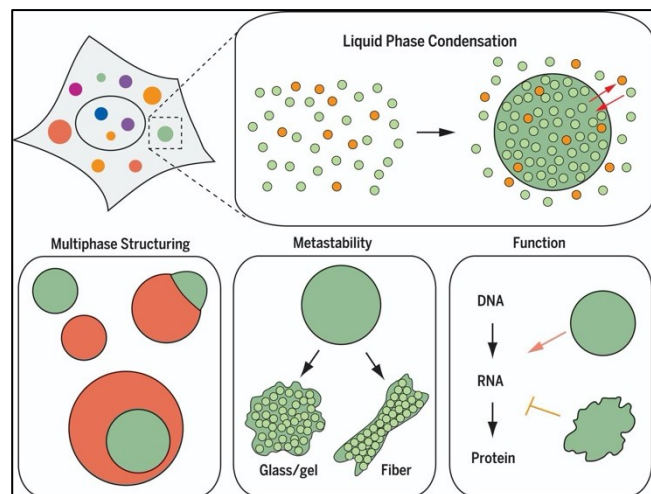


Figure 1. Schematic view of a eukaryotic Cell showing different biomolecular condensates: Different types of Biomolecular condensates are shown here. Some of them are specific to cell type but are represented here for knowledge. For instance, RNA transport granules are specific neuronal cells. (Banani *et al.*, 2017)

These compartments usually remind of lipid bilayer membrane partitioning inside and outside of the cell and maintain differential concentration of proteins and metabolites (Banani *et al.*, 2017). In 1899, researcher Edmund Wilson proposed that protoplasm in a cell forms phase separated mixture globular objects (Wilson, 1899). Lately, a decade ago, phenomenon of liquid-liquid Phase separation (LLPS) was discovered to rethink our idea about cellular organization. LLPS is a process by which a homogeneous liquid phase of proteins or nucleic acids or mixture of both, de-mix to form two distinct phases, condensed phase that is enriched for the macromolecules and another phase that is depleted of the same macromolecules (Li *et al.*, 2012). These

membrane-less compartments are formed by liquid-liquid de-mixing induced by specific trigger. The membrane-less compartments are also called as biomolecular condensates or droplets due to their condensed liquid like behavior. Most familiar ones are germ granules or Nucleoli, Stress granules, P granules, Processing bodies or P bodies and Cajal bodies (Banani *et al.*, 2017). The interactions driving phase separation are multivalent due to their low complexity domains of the RNA binding proteins within the condensed phase (Li



et al., 2012). Spontaneous phase separation is a particular ability of multivalent macromolecules that contain intrinsically disordered regions (IDRs) (Bentley, Frey and Deniz, 2019). Condensates formed by LLPS regulate numerous biological processes from transcription, translation to synaptic activation of receptor, then downstream signaling, hence defined as ‘liquid information flow’.

Figure 2. Liquid-liquid phase Separation in in cells:

Biomolecules assemble through regulated phase separation within cells in to condensed liquid like structures and are highly dynamic because of movement of molecules in and out of these structures. Physicochemical properties of their components give rise to multiphase structuring and solid-like states. The central dogma is disturbed by the liquid condensates that affect the flow of information (Shin and Brangwynne, 2017).

Membrane bound organelles organize their machinery by regulated transport of molecules through lipid layers, whereas biocondensates surface acts as an interface between internal and external that allows dynamic exchange of molecules (Brangwynne *et al.*, 2009) (Mitre and Kriwacki, 2016). One would imagine ribosome as a stable RNP formed in correspondence to the evolution of translation machinery. Droplets are different from other protein organization in the way that liquid droplets are dynamic and exchange their contents with their external environment. It is quite interesting to know how these droplets maintain their steady state conditions in spite of the fast exchange rates of their constituents namely proteins and RNAs (Brangwynne *et al.*, 2009) (Li *et al.*, 2012).

DISORDERED PROTEINS AND LLPS

Several proteins contain regions of Low complexity Domains (LCDs) that are responsible for age related protein aggregation diseases. FUS is a prion-like protein that phase separates due to DNA Damage and stress (Patel *et al.*, 2015). These sequences with low complexity are not involved in membrane and scaffolding, however, are found to play key role in many cellular processes. This disordered region of proteins is called

Intrinsically Disordered Regions (IDRs) and acts as linkers between interaction domains (Dyson, 2016). These sequences carry out distinct functions as they fold upon their interaction with specific partners as in case of STAT2 upon its interaction CREB-Binding Protein (Wojciak *et al.*, 2009). Besides intermolecular interactions, their intramolecular interactions also play a vital role in predisposing their LLPS property, which is inflected by phosphorylation within its IDRs (Yang *et al.*, 2020)

The salient feature of IDPs is the enrichment of polar and charged amino acids in these protein on the surface (Romero *et al.*, 1997). This means the average proportion of hydrophobic and aromatic amino acids to the hydrophilic and polar, charged amino acids is lower which explains their tendency of unfolding (Dyson and Wright, 2005). Several RNA and DNA-binding proteins possess these LCDs that allow them to interact in various combinations under different conditions. IDRs containing amino acid repeats like RG, QN, and YG are responsible for their association in RNP granules, Stress granules and P-bodies (Nott *et al.*, 2015). Prion Domains (PrDs) are a class of proteins that contain Tandem Repeats (TRs) within their Low Complexity Domains (LCDs) and form heritable protein complexes through their conformational changes. PrDs possess significance at epigenetic level as they underlie the molecular basis of long-term memory in many eukaryotes like yeast, fruit flies, snails and mice too. Variation in TRs implies ambiguous features for its beneficial effects on cell-surface adhesion and transcription factor activities in yeast and canine skull morphology and its devastating role in development of degenerative diseases like Huntington's disease, myotonic dystrophy and Parkinson's disease by formation of pathogenic fibrils (Gemayel *et al.*, 2015) (Bergeron-Sandoval, Safae and Michnick, 2016). Rather than changing the biophysical properties of droplets, mutations in RNPs promote increased maturation of the droplets that has decreased mobility with pathogenic amyloid like fibrils. Higher the concentration of IDRs, higher, is the droplet maturation and enhanced fibrilization. At this point, specific RNAs might be essential to promote phase separation at lower concentration, which indeed prevents aberrant transitions into a solid state, indicating the therapeutic significance of RNA in regulating RNP granules and disease management (Guo and Shorter, 2015).

ROLE OF RNA IN LLPS

RNA and protein are co-synthesised as RNA synthesizes protein and protein synthesizes RNA. Their symbiotic co-evolution gives rise to RNPs (Lanier, Petrov and Williams, 2017). The critical roles of LLPS in biology postulates that RNP condensates are the first toolbox to study the material properties of cell structures. Protein interacts with RNA at their RNA Binding Domains (RBDs) including RNA Recognition Motifs (RRMs), hnRNAP K homology Domain and DEAD box Helicase Domain (Hentze *et al.*, 2018). It is realized that RBPs are more ubiquitous than we could imagine as there are at-least 1000 RBPs found to code for

mammalian genome until recent past (Singh, Ricci and Moore, 2014) (Dasti *et al.*, 2019). Their interactions with RNA give rise to complex networks, cueing their vitality in various cellular processes. RBPs bind RNAs in a non-selective manner to perform their functions in mRNA translation and degradation. IDRs of RBPs are representative of multifunctional RNA binding motifs which can bind a range of highly specific to non-specific RNA targets. Thus, it is even possible, that their interaction may lead to co-folding of their interacting partners to carry out their functions. RNA binding to RBPs shall be described in two ways based on their biological or intrinsic specificities. It is possible that intrinsically specific RNAs might bind less efficiently *in vivo* as they do not fall into their high affinity or specificity range of binding potential (Jankowsky and Harris, 2015).

RNA is a cue card in regulating the viscoelasticity and dynamics of the condensates (Guo and Shorter, 2015). The interactions involving RNA might even be non-specific. The concentration of RNA is critical in promoting or dissolving the condensates. That is, higher concentration of RNA might often inhibit phase separation. (Lin *et al.*, 2015) Presumably, RNA sequence, secondary structure, length, charge distribution, and pattern of RBP binding sites along the mRNA are the factors that contribute to the effect of RNA in LLPS. Understanding the effect of these factors precisely shall benefit in elucidating the biogenesis of membraneless organelles which in turn provides valuable insights for designing therapeutic RNA to reverse the pathogenic fibrils formed by FUS, TDP-43 or hnRNPA1 in neurodegenerative diseases resulting in aberrant accumulation of RNP granules (Patel *et al.*, 2015).

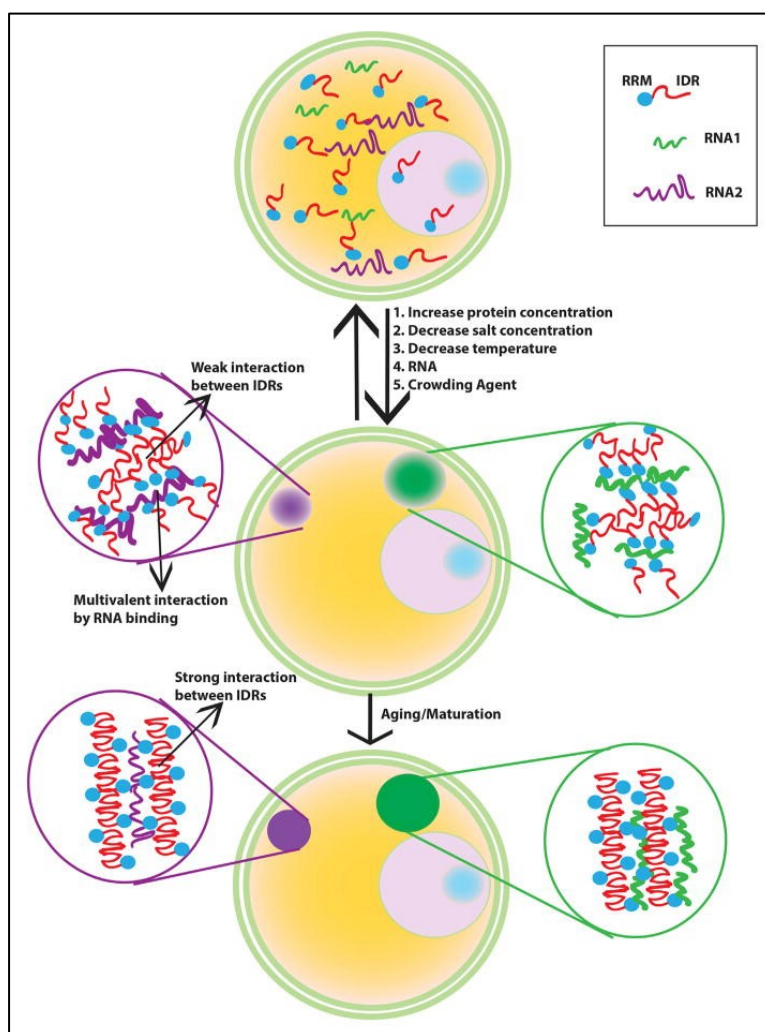


Figure 3. Formation and maturation of RNP granule: Proteins in RNP granules often contain IDRs and RRM. Different factors aid to the formation of granules among which RNA independently regulate the material properties of the granules. The initially separated phase consists of weaker interactions and mature over time in to a more solid-like structures where the interactions between IDRs becomes stronger (Guo and Shorter, 2015)

RNA-protein nanocondensates are multicomponent phase separated droplet. Some RNAs constitute the core and acts 3D matrix. On the other hand, some RNAs constitutes the shell component that is equivalent to 2D lipid bilayer, with the potential additional ability of informational content. The intra-droplet was previously observed to have stable core and dynamic shell which is also seen as a common feature of RNP granule. Nucleolus is a multi-layered structure that facilitates the assembly-line of rRNA processing, in which nascent rRNA transcripts are sequentially processed at specific compartments and transported from nucleolus to cytoplasm for ribosomal assembly. Similar to nucleolus, stress granules (SGs) exhibit multi-layered and its assembly and disassembly is of great biological significance. SGs showcases a highly cooperative assembly of molecules and very sensitive to small changes in interactions (Gasior *et al.*, 2019) (Jain *et al.*, 2016)

RNP assembly is characterized by surface recruitment and RNA concentration. This property confers increased stability to the core that allows adsorption of particles only on the surface like Pickering emulsion (Tauber, 2019). Surface recruitment regulates the interactions by enhancing stability against thermodynamic process favoring formation of larger droplets. Different terminologies like Ostwald ripening, coalescence and fusion represent the emergence of larger droplets from smaller ones (Wurtz and Lee, 2018) (Bentley, Frey and Deniz, 2019). One essential attribute of surface recruitment in RNPs may be that RNA surfaces are expected to be capable of promoting intermolecular interactions of localized RNAs resulting in interaction between donor and acceptor cognate-code guide RNAs for tethering inter-condensate interactions.

Besides influencing the biophysical properties of condensates, RNA may determine the specificity of its molecular composition. Nuclear speckles are RNP granules that colocalize with lncRNA *MALAT1* and are thought to be a storage site for splicing factors. Active genes are organized around nuclear speckles and so inhibition of transcription causes coalescence of nuclear speckles. Paraspeckles are interesting paradigm of LLPS, that are always found in adjacent to nuclear speckles. Paraspeckles are enriched with lncRNA *NEAT1*. More than 30 RBPs are harbored by paraspeckles including RBM14 and FUS. Nucleation of large number of RBPs by NEAT1 leads to collective binding of primary mi-RNAs, most of which reside in pre-mRNAs, that are to be processed at or near nuclear speckles. Thus, RNA processing events interplay between paraspeckles and nuclear speckles (Xiao and Xiang, 2019).

CAPTURING RNP COMPLEXES FOR CHARACTERIZATION

Characterizing RNA-protein interaction is complicated for many reasons. Identification of such interactions is important yet at the same time, challenging due to the limitations in the currently available methods of isolation and analysis. In general, studying the RNPs demands customization of every step involved in the experiment in order to acquire more reliable data. This includes crosslinking of the interactions, lysis methods and capture of complexes followed by library preparation. (Ramanathan, Porter and Khavari, 2019) One of the preliminary steps in isolating RNP complexes is crosslinking, which is the nub that leads to false interpretation either due to under-fixing or over-fixing. Beyond the physical factors, nature of complexes targeted would also contribute to efficiency of crosslinking.

UV CROSSLINKING

For RNP analysis, in-vivo UV-crosslinking followed by immunoprecipitation (CLIP) (Ule *et al.*, 2003) and its subsequent modifications (Lee and Ule, 2018) have led the way to expand our knowledge on RNA metabolism. In vivo UV light crosslinking forms covalent bonds between RNAs and directly bound proteins

at zero distance (Hockensmith *et al.*, 1986). The need for direct juxtaposition of photo-reactive groups (aromatic amino acid side chains and nucleic acid bases) at the RNA–protein interface makes it the method of choice for the analysis of direct RNA-contact sites. Such level of specificity, however, introduces constraints both to other types of indirect interactions (such as the sugar-phosphate backbone or double stranded RNA) and most importantly for the crosslinking of larger or higher order complexes. Moreover, the standard UV-light crosslinking has to be performed at 4°C to avoid UV-induced signal transduction thus changing the material state of intracellular phases. Notwithstanding these caveats, this technology has opened the field of RNA-protein interactions as will continue to do in the future. UV crosslinking is less efficient especially when interactions are weaker. Hentze and Beckmann’s groups reveal only 5 % RBPs can be crosslinked by UV. Additionally, its irreversibility makes it an incompatible method for many studies. (Urdaneta and Beckmann, 2019). UV crosslinks only Protein-RNA interactions, which may not be very useful while studying membraneless organelles which are generally composed of several proteins and Nucleic acid components interacting directly or indirectly.

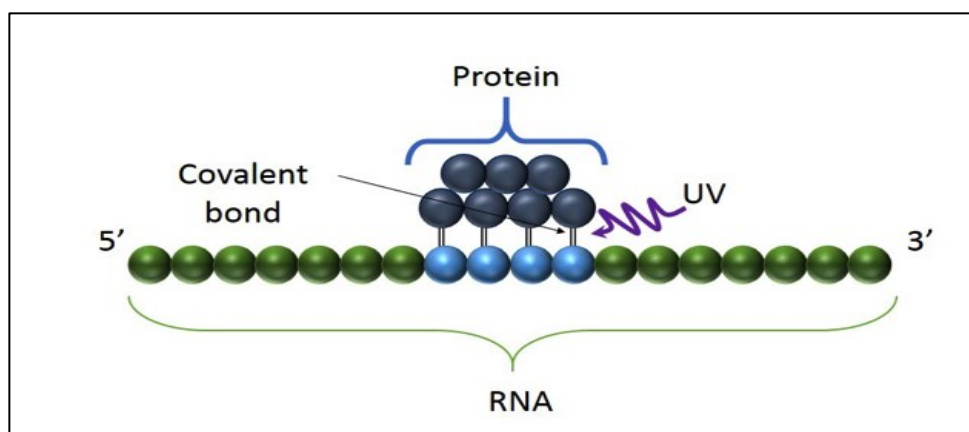


Figure 4. UV crosslinking in RNA: UV light creates covalent bonds between vicinal proteins and RNAs. They are crosslinked only at the direct sites of contact (<https://www.creativebiomart.net/resource/principle-protocol-crosslinking-and-immunoprecipitation-clip-388.htm>)

CHEMICAL CROSSLINKING

RNA-protein interactions can be studied with the help of several methods including Tat fusion assay, translational repression assay, frameshifting assay and yeast three-hybrid assay (Niranjanakumari *et al.*, 2002). However, these methods do not identify native interactions. Therefore, it is crucial to crosslink their native interaction states in order to recognize the binding partners and the biological significance of such interactions. UV crosslinking is an *in vivo* crosslinking method requires longer exposure that ultimately allows in redistribution of components and crosslinking of UV-damaged molecules. cDNA microarrays along with RNP

tagging was developed to identify the RNA species in endogenous complexes. Despite being useful, this method comes with serious risk of post-lysis association or dissociation of macromolecules that hampers the correct interpretation of results. Therefore, it is essential to freeze the interactions rapidly to prevent reassembly of such sticky components in the cell. Chemical crosslinking agents are useful which mostly form reversible crosslinks making subsequent characterization possible.

Aldehydes are well-known compounds for their ability to crosslink macromolecules in vivo (Hopwood, 1969). Among aldehydes, formaldehyde found widespread application in fixation of cell structures for microscopy and other protocols like ChIP and RIP to study protein-nucleic acid interactions.

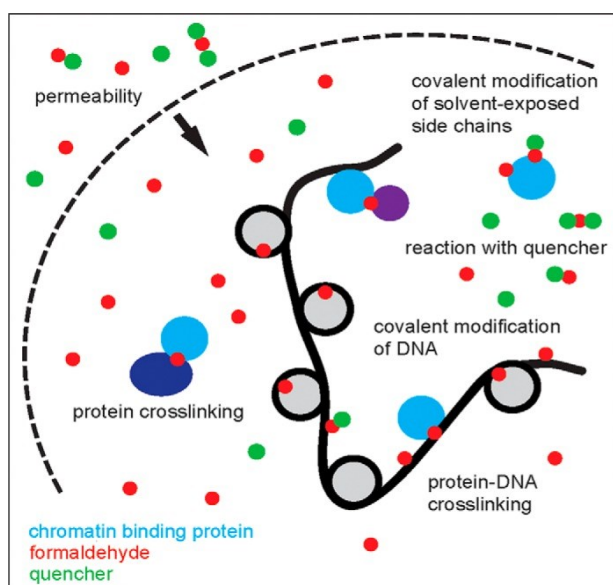


Figure 5. Graphical model of formaldehyde mediated crosslinking: Formaldehyde (red circles) easily penetrate through cell or nuclear membrane (dashed arc) and crosslink the macromolecules (blue and cyan), modifying the exposed groups on the macromolecules. Likewise, quenchers Tris or glycine (green circles) also permeate through membrane easily and quench free aldehyde groups (Hoffman *et al.*, 2015).

Apart from formaldehyde, acetaldehyde, glutaraldehyde, methyl and phenyl glyoxal, mono-, di- and tri-glycodialdehyde, acrolein, crotonaldehyde, α -hydroxy- adipaldehyde, malonaldehyde, malialdehyde and succinaldehyde are also known to crosslink cellular components. Although, most of them are convincing for electron microscopy related fixation, only formaldehyde and glutaraldehyde have shown excellence in their ultrastructure fixing ability that allow for their use in biochemical characterization studies (Niranjanakumari *et al.*, 2002).

FORMALDEHYDE

Due to its smaller size and bifunctional property, formaldehyde is able to diffuse rapidly into cells and forms a network of macromolecular adducts involving protein, DNA and RNA that are within 2 Å (Brent W. Sutherland, Judy Toews, 2008). These crosslinks are formed by covalent interactions between the molecules and require higher temperature for reversal. Formaldehyde reacts with the nucleophilic group of the proteins via covalent interaction to form methylol adducts. The methylol adducts lose water molecules to become Schiff's bases that contain an imine group. Further, the methyl group of Schiff's bases forms a methylene bridge between itself and the nucleophile on another macromolecule such as RNA or DNA or protein, resulting in the formation of a crosslinked product (Feldman, 1973) (Stancheva *et al.*, 1997). Applying the same chemical principle, the excess formaldehyde in the reaction can be quenched with glycine

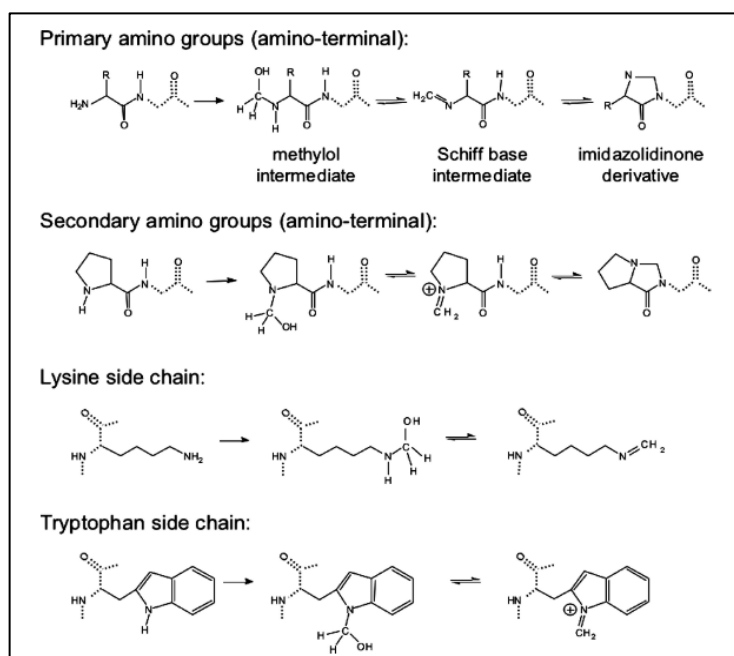


Figure 6. Scheme of formaldehyde crosslinking chemistry: In the first step formaldehyde forms methylol adduct or Schiff's base by reacting with primary or secondary amino groups. Following the formation of Schiff's base, the reaction proceeds to form a cyclic derivative called imidazolidinone (Brent W. Sutherland, Judy Toews, 2008).

solution. Thus, the formation of reversible crosslinks yet strong enough for characterization studies is a major interest to biologists. Perhaps, due to their self-polymerizing property, there might be some formaldehyde aggregates whose reactivities and distance-spanning capabilities are unclear (Hoffman *et al.*, 2015).

GLUTARALDEHYDE

In 1963, for the first time, Sabatini used glutaraldehyde as a fixative for electron microscopy (Sabatini, Bensch and Barnett, 1963). Glutaraldehyde is a linear dialdehyde with a 5-carbon chain, extremely soluble in water as well as organic solvents. Its dialdehyde group makes it a more efficient crosslinking molecule in comparison to FA. Glutaraldehyde reacts with amine, hydroxyl, and thiol groups in the reactants to form amine,

acetal and thioacetal bonds. The presence two aldehyde groups allow it to react with the macromolecules to form intramolecular as well as intermolecular crosslinks which are both thermally and chemically stabler. The intramolecular crosslinking is more appreciative for it can stabilize the single molecule stabilizing its structural configuration. GA fixation has stronger influence on the molecules both directly and indirectly when compared to FA (McKenzie, 2019). One study shows that different types of purified proteins in the mixture could be crosslinked in 10 seconds, completely (Ouimet *et al.*, 2018). Despite FA having higher diffusion coefficient than GA, higher concentration of FA is required to achieve the same level of crosslinking as of GA. Apart from all the meritorious effects of GA, it is quite unclear to what extent affects the location, chemical composition and structural configuration of proteins. The crosslinking abilities of GA is a little compensated by FA even though it has found its supremacy over other fixatives with higher crosslinking abilities.

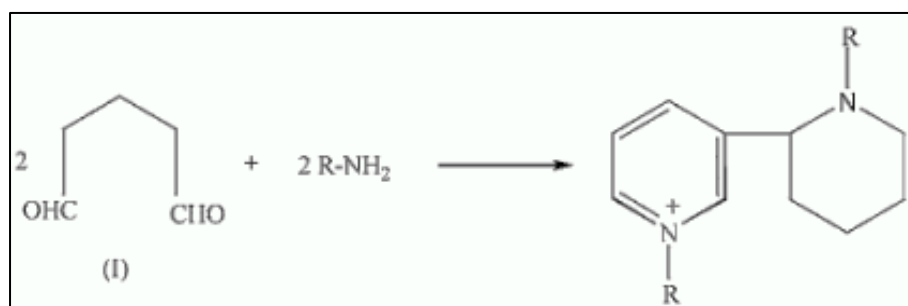


Figure 7. Glutaraldehyde crosslinking of proteins: A proposed chemistry of glutaraldehyde crosslinking shows formation of quaternary pyridinium compound.

Lysine is the key amino acid involved in crosslinking proteins by dialdehydes. GA exists in equilibrium with hemiacetal form and hemiacetal polymers at acidic pH and increases in the unsaturated polymer length with increase in pH. Hence, GA crosslinking is usually to done at basic pH. Similar to formaldehyde, glutaraldehyde is shown to react with the primary amines forming Schiff's Bases however their extreme stability at alkaline pH contradicts principle of Schiff's mechanism. Alternative mechanisms such as Michael-type addition of conjugate protein amino groups to unsaturated oligomers of glutaraldehyde. Another important mechanism postulated was the formation of quaternary pyridinium compounds due to the dimerization of amino groups. Despite of having different mechanisms proposed, reaction of glutaraldehyde with proteins is obscure (Modenez *et al.*, 2018).

DIFFERENCE BETWEEN FA AND GA

Formaldehyde is less permeable than glutaraldehyde through plasma membrane and that makes the former a better fixative as it does not fix the first layer of the tissue. Rather, glutaraldehyde penetrates faster and

immediate fixes the first layer of tissue leading to subsequent blockage. (Vassar *et al.*, 1972) Such differences are due to the fact that FA is a highly hydrophilic molecule when dispersed in water and its major form (>90%) is methylene-glycol or methane diol which is stabilized by hydration shell of 12 molecule of water. It does not have any specific membrane carrier and its passive diffusion requires, therefore, is required in high concentrations (4%FA= 1.44 Molar) to be effective for cultured cells. It might use aquaporins as carrier in facilitated diffusion, it would be outcompeted by water.

Conversely, glutaraldehyde in water is >70% in the form of a cyclic-hemiacetal (Whipple and Ruta, 1973) resembling a reducing sugar in nature. This form could therefore potentially use sugar transporter to follow its chemical gradient as facilitated diffusion inside the cell. Since the fixation-time depends on plasma-membrane permeability of crosslinking agent, formaldehyde is required at higher concentration as competed by water through aquaporins while glutaraldehyde diffuses faster encountering no competition at its sugar transport channels. In fact, the concentrations of GA used to obtain efficient cell-fixation are usually not more than 1% which is equivalent to a concentration of hemiacetal of 7-10 mM. The fast-crosslinking chemical mechanism of GA ranging from seconds to minutes is based on the attack to nucleophilic groups. If the nucleophilic-group is an amine, dihydro-pyridines are formed as end products which are rapidly oxidized to pyridinium cations, whereas nucleobase as nucleophilic group forms tetrahydro- pyranes (Johnson, 1993).

QUENCHING

One of the key steps in fixation process is quenching excess or unreacted formaldehyde at the end of the reaction. Basically, it is to arrest the formaldehyde from further crosslinking the molecules in the sample. The chemical mechanism follows the same principle of amino group of Glycine binds to the unreacted aldehyde group and forms the Schiff's bases that should be discarded away. It is also important to optimize the time of quenching as it can cause reversal of crosslinking over longer time (Hoffman *et al.*, 2015). However, it is not as quick as the crosslinking mechanism, but one can expect loss of weaker crosslinks. As amine group is the player of the reaction, compounds like Tris, which contains amine group could also be de-crosslinker (Cordes and Jencks, 1962).

The strong covalent interactions are important to prevent post-lysis random associations of molecules yet is challenging to bring a compromising reversal state in order to correctly characterize the complexes. Therefore, quenching and reversal are small but major steps to be optimized in order to avoid weak treatments that results in failure of demodification or strong treatments that results in hydrolysis of crosslinked components itself (Niranjanakumari *et al.*, 2002).

Having seen several possibilities of crosslinking RNA-protein interactions, the methods are strictly dependent on the model system, target and the goal of the study. Approaches like RNP tagging that can specifically capture the component of any given complex are often less feasible as lysis causes a cluttering of cellular components after which it becomes difficult to expect high specificity or retention of original interactions. Therefore, fixation of the cell is the first and foremost solution if not to avoid disintegration of the weak but natural complexes (Tenenbaum *et al.*, 2002) (Niranjanakumari *et al.*, 2002). However, fixation cannot be specific and results in crosslinking of whatever that applies to the chemistry. Perhaps, the only step where to expect a minimum specific is the immuno capture of the complexes. But it is practically more difficult due to the enrichment of abundant housekeeping proteins like actin, GAPDH and HSP 90 that non-specifically purify with the beads. Even our experiments show non-specific association of GAPDH mRNA in RNA extracted from crosslinked immunoprecipitated complexes. More perplexing is that such non-specific background is not always detected in control samples (Kast and Klockenbusch, 2010).

The temporal partition between specific and stable anchoring of RNAs have dwell-time of >15 secs up to 250 secs while 'non-specific/transient' 1 sec to 10 secs; thus, the difference between stable and transient association of RNAs with RNPs is of the order of 10x. In response to stress, mRNAs are found to associate both stably (~250 s) and transiently (~10 s) with stress granules and P-Bodies. Nuclear paraspeckles and cytoplasmic condensates stress granules have been recently shown to be structurally and functionally connected at least in their proteome composition, whereby SGs regulate PSs assembly in response to stress via rapid exchange of protein components within a continuum as required for temporal control of cellular stress response (Mohammad Lellahi *et al.*, 2018) (An, Tan and Shelkovnikova, 2019). A necessary requirement to follow such dynamical compositional identity, using proteins as handles for their isolation, is to develop technologies that allow for fast in-vivo crosslinking methodologies to maintain and capture the complete picture of RNA-protein interactions as required for reconstructing the high temporal exchange dynamics. In this context, UV-crosslinking based Cross-linking Immunoprecipitation (CLIP) technologies is limited in its applicability to proteins that are in direct contact with RNA (i.e., RBPs) being ill-suited to study proteins that interact with RNA indirectly within condensates.



RESULTS

HIGH THROUGHPUT IMAGING TO IDENTIFY THE BEST CROSSLINKING CONDITIONS

In order to investigate short crosslinking kinetics of cytosolic protein components, high throughput imaging was performed under 10 x magnification (Olympus 10x NA 0.95) with a PerkinElmer Operetta High content Imaging system by trying several concentrations of formaldehyde and glutaraldehyde. For this purpose, U2OS cells stably expressing GFP-G3BP1 were used. To start with, prior to fixation, the cells were stained with Hoechst in growth medium for 10 minutes at 37°C/5 % CO₂, given that the optimal staining of nucleus was separately checked. The medium was then removed, and the cells were washed with HBS. Cells were subjected to fixation with selected concentrations of freshly prepared formaldehyde or glutaraldehyde solutions in HBS for one minute. The concentrations used were 0.5, 1, 2, 4% for formaldehyde and 0.01, 0.05, 0.1 % for glutaraldehyde. After one minute, the fixative solutions were removed and the cells were quickly rinsed with TBS (Tris buffered saline, pH 7.8) and images were acquired with 10 x objective. In order to identify the most efficient fixation, cells were treated with lysis buffer containing 0.6 % DDM and 0.1 % SDS in 20 mM Tris, pH 7.8, 150 mM NaCl and 2 mM EDTA for 3 minutes and the images were similarly acquired with 10x objective. (FIGURE 8 PANEL A) shows that the fluorescence of GFP-G3BP1 increased with increasing concentration of the formaldehyde. At the higher concentration of (4%FA), a significant number of cells with intact cytoplasm and nucleus were visible having significantly higher fluorescence than cells fixed with lower concentration. Similarly, glutaraldehyde showed effective crosslinking for one minute with increasing concentration as demonstrated by the increase in the number of intact cells after lysis treatment with DDM/SDS (FIGURE 8 PANEL B). These results show that increasing the concentration of formaldehyde or glutaraldehyde significantly improved the fixation of cells in the short-selected time window.

Next, a lower concentration of formaldehyde (0.5-1%) combined with the (0.05-0.1%GA) was used for crosslinking in one minute similarly followed by 3 minutes lysis in DDM/SDS buffer. It was shown that after treating cells with lysis buffer, (0.5 % FA+0.05) % GA and (1%FA+0.1%GA) were more efficient than FA or GA alone as evident from the presence of the respective increased numbers of intact cells with cytoplasmic GFP and Hoechst-stained nuclei (FIGURE 8 PANEL C). In the last part of results section, results from screening of compounds other than FA and GA are included.

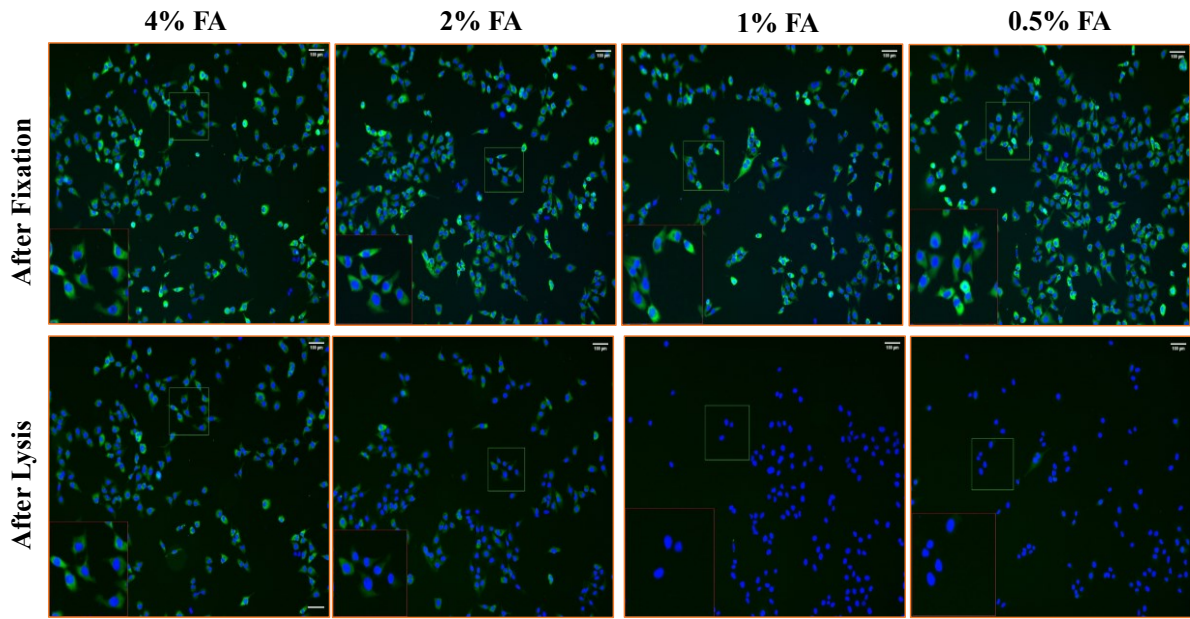
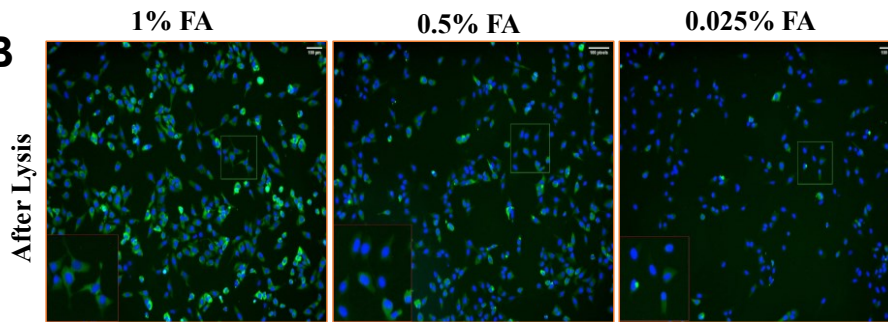
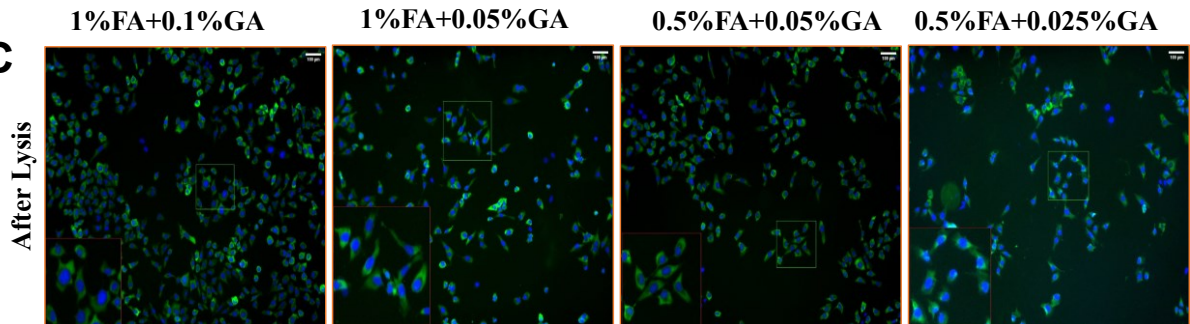
A**B****C**

FIGURE 8. HIGH THROUGHPUT IMAGING OF TITRATION OF CONCENTRATION OF FORMALDEHYDE AND GLUTARALDEHYDE IN ONE MINUTE FIXATION: **PANEL A** shows representative images U2OS GFP-G3BP1 fixed with different concentrations formaldehyde (0.5%), (1%), (2%) and (4%) from left to right. **PANEL B** shows representative images U2OS GFP-G3BP1 fixed with different concentrations glutaraldehyde (0.025%)-left, (0.05%) -middle, (0.1%)-right. **PANEL C** shows representative images of U2OS GFP-G3BP1 fixed with different combinations of formaldehyde and glutaraldehyde (0.5%FA+0.025%GA)-left, (0.5%FA+0.05%GA)-middle, (0.5%FA+0.1%GA) -right. The images were acquired after 3 minutes lysis with DDM+SDS lysis buffer under 10 x objective. Scale bar is 100 μ m

FRAP- A REAL TIME ANALYSIS TO DETERMINE THE RESULTANT MOBILITY OF THE GFP-G3BP1 CROSSLINKED-COMPLEXES

FRAP analysis was carried out in U2OS GFP-G3BP1 to confirm the fixative conditions determining crosslinking as assessed by limited mobility of GFP-G3BP1 within one minute. Amongst the fixation conditions previously screened by HT, (4%FA), (0.5%FA+0.05%GA) and (1%FA+0.1%GA) were selected as final candidate fixatives for FRAP analysis. Live cells were used as control for recovery after photobleaching establishing the parameters of FRAP for comparative analysis on fixed cells. For bleaching, Region of Interest (ROI) was sized 3 μm in diameter. A total of 393 seconds (average of 6.4 minutes) with 490 frames of images were collected including 20 prebleach and 470 post bleach images. Live cells recovered over 100 % of the initial fluorescence and the mobile fraction present was 0.96. Under the same conditions, 1-minute fixation with freshly prepared crosslinking solutions was performed followed by quick washing with TBS: cells topped with HBS were used for imaging. The cytoplasmic GFP-G3BP1 fixed with (4%FA) showed steady recovery of fluorescence after bleaching indicating its less effective in immobilizing the molecules. On the other hand, cell fixed with the two combinations of FA+GA (0.5%FA+0.05%GA) and (1%FA+0.1%GA) showed significantly slower recovery of fluorescence after photobleaching thus showing stronger crosslinking ability (FIGURE 9 PANEL A). Further analysis of FRAP data estimated the percentage recovery of fluorescence in the fixations: 4%FA recovered: 76 %, (0.5%FA+0.05%GA): 47.6 % and (1%FA+0.1%GA): 25.3 % (FIGURE 9 PANEL B). In addition, the mobile fraction of GFP-G3BP1 present after fixation were calculated to be 0.61, 0.30 and 0.14 respectively as compared to 0.96 in live cells (FIGURE 9 PANEL C). Thus, FRAP experiments presented a real time analysis of immobilization efficiency of the three fixation conditions on cytoplasmic GFP-G3BP1. Together with high throughput Imaging, FRAP analysis indicated the choice of using glutaraldehyde in combination with formaldehyde to achieve effective crosslinking within the selected time window.

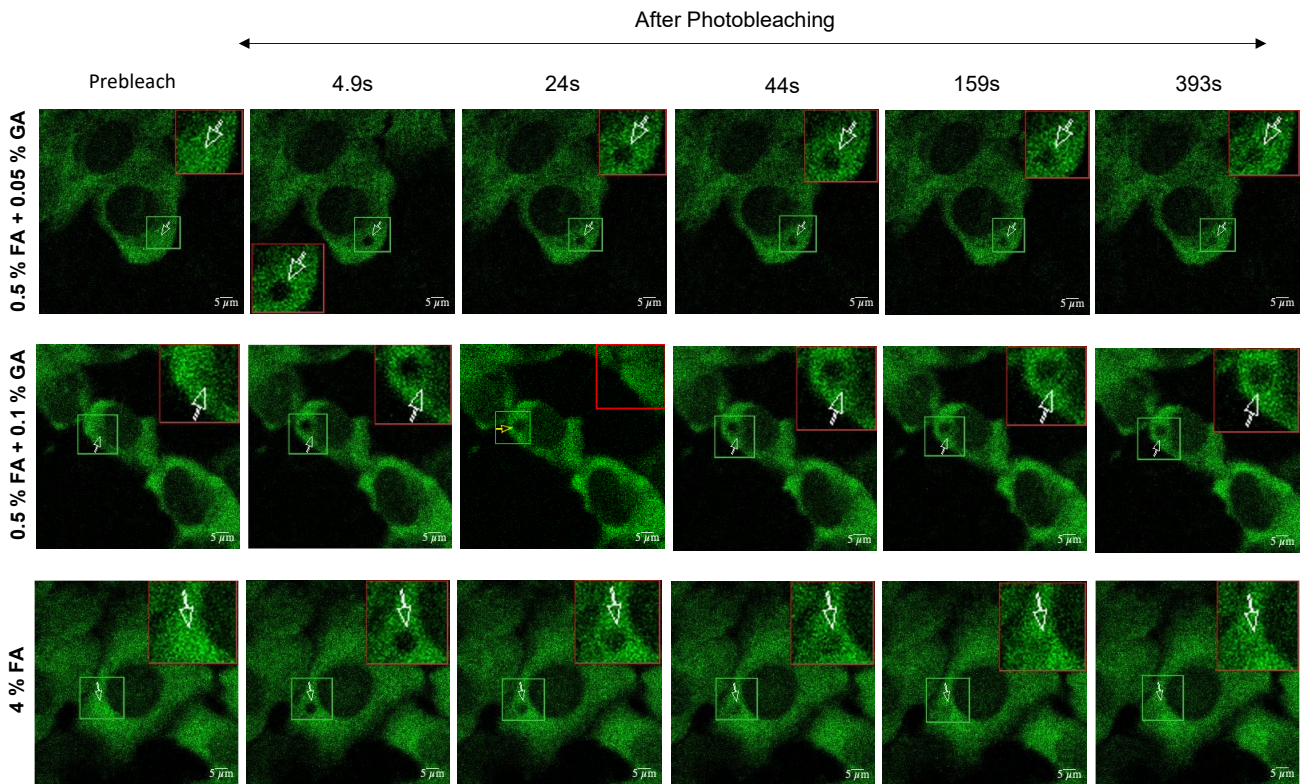
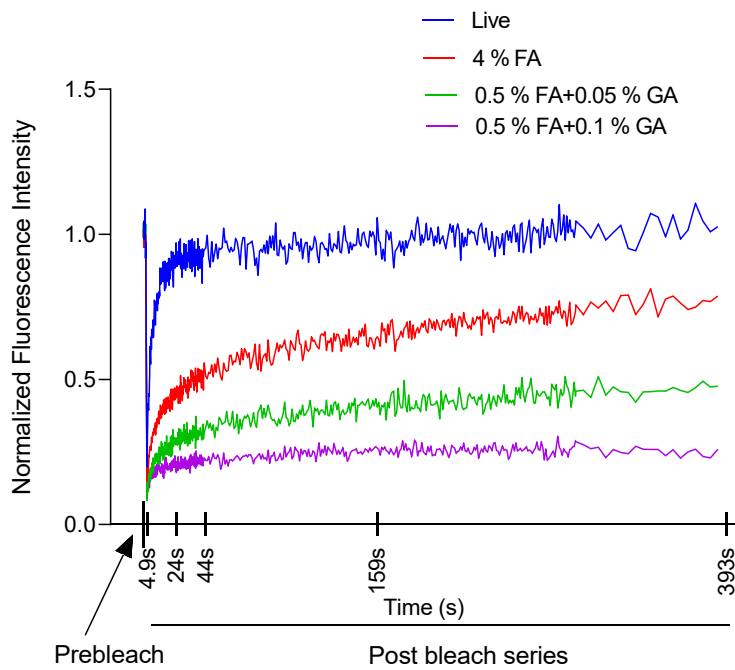
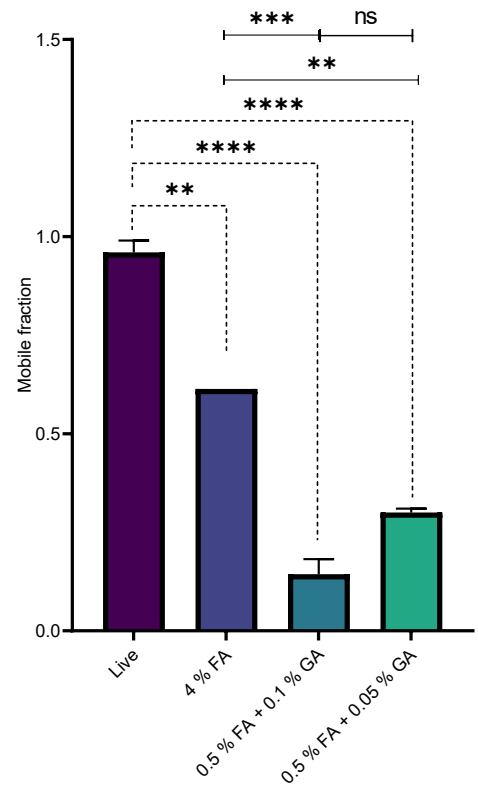
A**B****C**

FIGURE 9. FRAP ANALYSIS TO VALIDATE CROSSLINKING EFFICIENCY OF THE FIXATIVES FOR CYTOPLASMIC GFP-G3BP1: **PANEL A**-Representative images of U2OS GFP-G3BP1 in the order of first prebleach image, and five images at indicated time points after photobleaching (post bleach 1 t/1-200 1-4.9 s, postbleach 1 t/100-200 2-24 s, postbleach 2 t/200-200-44s, postbleach 2 t/125-250-159s, postbleach 3 t/20-20-393s). White arrows indicate the ROIs. Scale bar is 5 μ m. **PANEL B**- The graph shows the normalized fluorescence intensity against time after fixation and in live cells. The intervals marked on the x axis are relative to the images presented above. **PANEL C**-The mobile fraction present in each fixation and living cells as estimated from individual the curve fits (U2OS GFP-G3BP1: live, n=2; fixed samples, n=3 each). Data are mean \pm SEM and statistical significance was assessed by Ordinary one-way ANOVA test

BIOCHEMICAL ANALYSIS TO VALIDATE THE FIXATIVE CROSSLINKING CONDITIONS AS DETERMINED BY SDS-PAGE OF GFP-G3BP1 HIGH-MOLECULAR WEIGHT COMPLEXES

We then tested if the rapid fixation conditions used above could form covalent intermolecular contacts preserving the selected complexes to be subsequently captured by immunoprecipitation. First, we analysed the extracted samples by SDS-PAGE followed by western-blot of GFP-G3BP1 to check for the presence of higher-molecular weight complexes with respect monomeric species. U2OS GFP-G3BP1 cells were fixed with different concentration of FA and the combination of FA+GA and extracted by lysis with DDM/SDS lysis buffer followed by sonication and centrifugation AT 13000 x g RCF. The obtained supernatant samples were analysed by SDS-PAGE-Western blot. The results showed a modest increase in high molecular complexes with respect to monomer with increasing concentrations of FA (FIGURE 3 PANEL A). On the other hand, the combination fixatives (1%FA+0.1%GA) and (0.5%FA+0.05%GA) showed a significant decrease in the monomer band accompanied by a significantly higher amount of crosslinked products containing G3BP1 formed by combined FA+GA. Such crosslinked products were efficiently extracted by sonication as indicated by increasing high molecular weight smears seen in lanes 5 and 6 of FIGURE 10 A. This observation not only confirmed the possibility of achieving effective crosslinking of cytoplasmic protein G3BP1 in 1 minute but also the suitability of DDM/SDS lysis buffer and sonication to extract the complexes from FA+GA fixation for biochemical analysis.

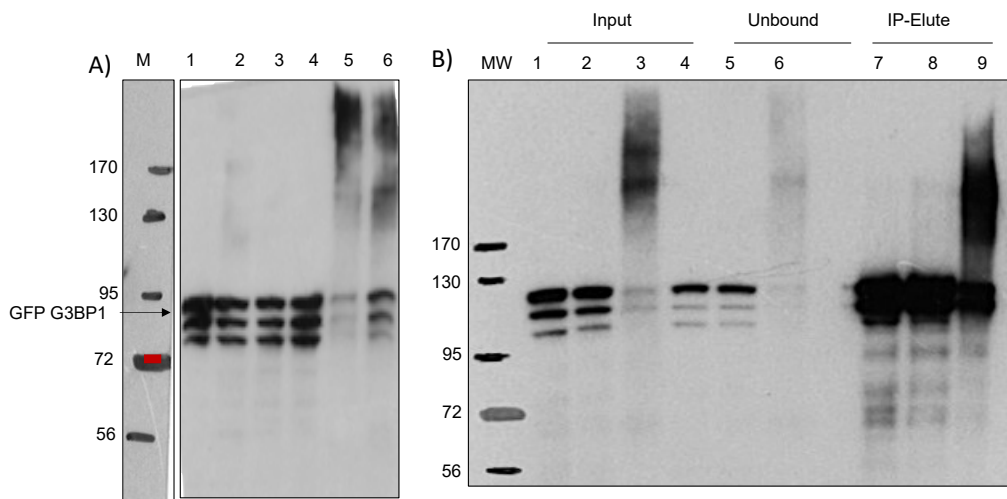


FIGURE 10. BIOCHEMICAL ANALYSIS TO CONFIRM PROTEIN CROSSLINKING-SDS-PAGE AS A READ OUT:

PANEL A) U2OS GFP-G3BP1 cells were crosslinked for 1 minute with different fixatives (or without crosslinking) and then lysed in +SDS lysis buffer followed by sonication and centrifugation. The lysate supernatants were prepared with 2x Laemmli buffer and loaded to 12% SDS PAGE for Western Blot and probed with anti-GFP. The samples were loaded in the following order: **PANEL A: M)** protein marker; **Lane 1)** (Unfixed); **Lane 2)** (4%FA); **Lane 3)** (2%FA); **Lane 4)** (1%FA); **Lane 5)** (0.5%FA+0.1%GA); **Lane 6)** (0.5%FA+ 0.05%GA). **PANEL B:** Immunoprecipitation of crosslinked complexes of G3BP1. The uncrosslinked and crosslinked cell lysates were immunoprecipitated with anti-G3BP1; the lysates (inputs for IP), unbound fractions and bound material (eluted by boiling for 5 minutes) were mixed with 2x Laemmli buffer, boiled for 5 minutes and analysed by 12 % SDS PAGE followed by western Blot for G3BP1. The samples were loaded in the following order: **Lane 1)** cell lysate of uncrosslinked cells; **Lane 2)** cell lysate of (0.5%FA); **Lane 3)** cell lysate of (0.5%FA+0.05%GA); **Lane 4)** unbound from uncrosslinked; **Lane 5)** unbound from (0.5%FA); **Lane 6)** unbound from (0.5%FA+0.05%GA); **Lane 7)** IP eluate uncrosslinked; **Lane 8)** IP eluate of (0.5%FA); **Lane 9)** IP eluate of (0.5%FA+0.05%GA)

In order to validate if these optimized conditions of fixation and lysis/sonication were compatible with immunoprecipitations of G3BP1 associated complexes, the extracted samples from crosslinked cells were subjected to specific immunoprecipitation using anti-GFP conjugated magnetic beads (GFP-trap). Firstly, SDS concentration in the samples was reduced to 0.05% by adding 1 volume of lysis buffer containing only 0.6%/DDM, followed by preclearing of the diluted lysates with protein A/G Dynabeads. Then, the precleared samples were subjected to GFP immunoprecipitation with the anti-GFP magnetic beads. The bound materials from the beads were eluted by boiling for 5 minutes in Laemmli buffer supplemented with beta-mercaptoethanol. SDS-PAGE followed by Western blot analysis of inputs unbound fractions and eluates was carried out. The crosslinked products were enriched in the respective eluates while only discrete monomers of G3BP1 band was enriched in uncross-linked eluates (FIGURE 10 PANEL B). These results are in agreement with high throughput imaging and FRAP analysis. Western blot analyses of crosslinked cell lysates followed by immunoprecipitation demonstrate the effectiveness of FA+GA combination fixative and its

compatibility for use in biochemical characterization of macromolecular complexes such as RNP condensates containing cytoplasmic proteins such as G3BP1.

YAP1 AS CYTOSOL-NUCLEAR PROTEIN

Recent studies showing YAP, cytoplasm localized co transcription factor forming dynamic condensates in response to hyperosmotic stress (Cai *et al.*, 2019). In addition to G3BP1, we wanted to test if the fixative/crosslinking conditions could be applied to YAP1 as a Transcriptional Coregulator shuttling from cytosol to nucleus in a controlled manner. Biochemical analyses were thus carried out under same conditions as used for G3BP1. The results were in agreement with the former showing that combination (0.5% FA+0.05%GA) being able to crosslink YAP1 in the cells effectively in one minute. Moreover, specific immunoprecipitation showed enrichment of YAP1 specific crosslinked products in their eluates thus corroborating with the results observed with former cytoplasmic protein GFP-G3BP1(FIGURE 11).

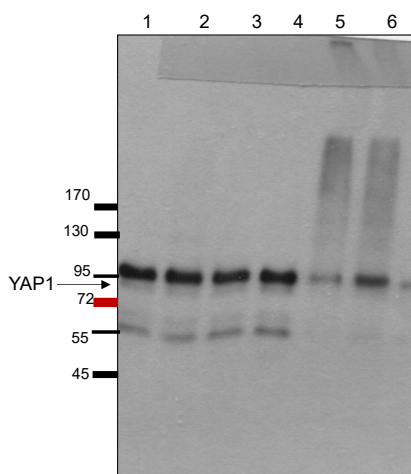


FIGURE 11: WESTERN BLOT TO CHECK CROSSLINKING OF YAP1 SPECIFIC COMPLEXES: HCT-116 FLAG YAP1 cells were crosslinked for 1 minute with different fixatives and then lysed in DDM+SDS lysis buffer followed by sonication and centrifugation. Brackets indicate crosslinked products represented by the higher smears on the blot. Uncrosslinked cells were lysed similarly by sonication and centrifugation. Clarified lysates were prepared with 2x Laemmli buffer and loaded to 12% SDS PAGE for Western Blot and probed with anti-YAP1. The samples were loaded in the following order: **M**) protein marker; **Lane 1**)(Uncrosslinked); **Lane 2**)(4%FA); **Lane 3**)(2%FA); **Lane 4**)(1%FA); **Lane 5**)(0.5%FA+0.1%GA); **Lane 6**)(0.5%FA+ 0.05%GA)

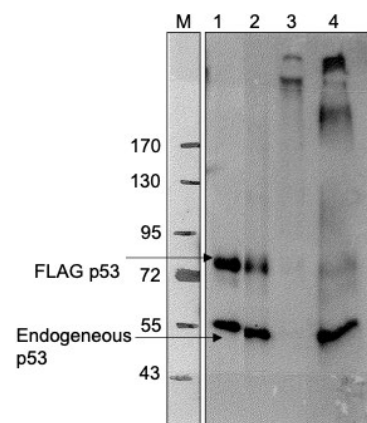
P53, A NUCLEAR-TF, AS A FURTHER VALIDATION OF SNAP-SHOT CROSSLINKING

As assessed for both GFP-G3BP1 and YAP, we wanted to analyze if the same biochemical extraction protocol could be used for a nuclear TF-protein such as p53. For this, we analysed wtp53 from HCT-116 cells with and without crosslinking after lysis/extraction as similarly assessed for GF3BP1 and YAP. Crosslinked HCT-116 cells were lysed with DDM/SDS lysis buffer followed by sonication and centrifugation at 13000 x g RCF. When analysed these lysates by western blotting, crosslinked cells showed low recovery of crosslinked products (FIGURE 12). Multiple experiments proved low recovery of crosslinked products. The cause of such lower recovery is attributable to the lack of solubilization: when the pellet from (1%FA+0.1%GA) fixation was analysed by western blotting, it was quite clear that most of the p53 was present in the insoluble pellet as evidenced also from the high degree of crosslinking (FIGURE 12-Lane 4). Therefore, it was clear that nuclear and cytoplasmic protein could not be extracted under same conditions using the same optimized snap-shot

fixation protocol. Therefore, we reinvestigated the optimized protocol by using a nuclear-GFP-tagged protein as a model-marker like GFP-G3BP1.

FIGURE 12. SDS-PAGE-WESTERN BLOT ANALYSIS TO CHECK FOR CROSSLINKED

COMPLEXES OF P53: HCT-116 FLAG p53 cells were crosslinked for one minute with different concentrations of FA and combinations of FA and GA, washed quickly with TBS and lysed in DDM/SDS buffer followed by sonication and centrifugation. Clarified lysates were prepared with 2x Laemmli buffer and loaded to 12% SDS PAGE for Western Blot and probed with anti-p53. The samples were loaded in the following order: **M**) protein marker; **Lane 1**) unfixed; **Lane 2**) UV fixed; **Lane 3**) (0.5%FA+0.05%GA); **Lane 4**) pellet from (0.5%FA+0.05%GA) solubilized by boiling in 2x Laemmli buffer and loaded to 12% SDS-PAGE.



GFP-FUS AS MODEL SYSTEM TO ANALYZE SNAP-SHOT FIXATION / CROSS-LINKING EFFICIENCY OF A NUCLEAR-MARKER

To check if the optimized short crosslinking protocol works differently for nuclear protein, we used HeLa GFP-FUS cells with different concentrations of formaldehyde and combinations of formaldehyde and glutaraldehyde as previously optimized for GFP-G3BP1. High-content screening was similarly done using NP40/SDS as lysis buffer which gave better extractability as compared to DDM/SDS for nuclear p53. At first, cells were stained with Hoechst and fixed for 1 minute with formaldehyde (0.5, 1, 2, 4%) and combinations (0.5%FA+0.1%GA) and (0.1%GA), and the images were collected under 10 x objective. Next, the cells were subjected to lysis with 20 mM Tris, pH 7.8, 150 mM NaCl, 2 mM EDTA, 0.6%NP40 and 0.1%SDS for 3 minutes, after which lysis buffer was aspirated and TBS added: images were then similarly acquired by topping in HBS. In comparison to 0.5, 1 and 2%FA, cells fixed with 4%FA showed more intact GFP containing nuclei (FIGURE 13). Combinations of FA and GA demonstrated to be more efficient as compared to FA alone as indicated by their GFP signal in the nuclei. Thus, according to the observations from high throughput imaging, GA based fixation was necessary for achieving maximum fixation of nuclear-protein marker within one minute.

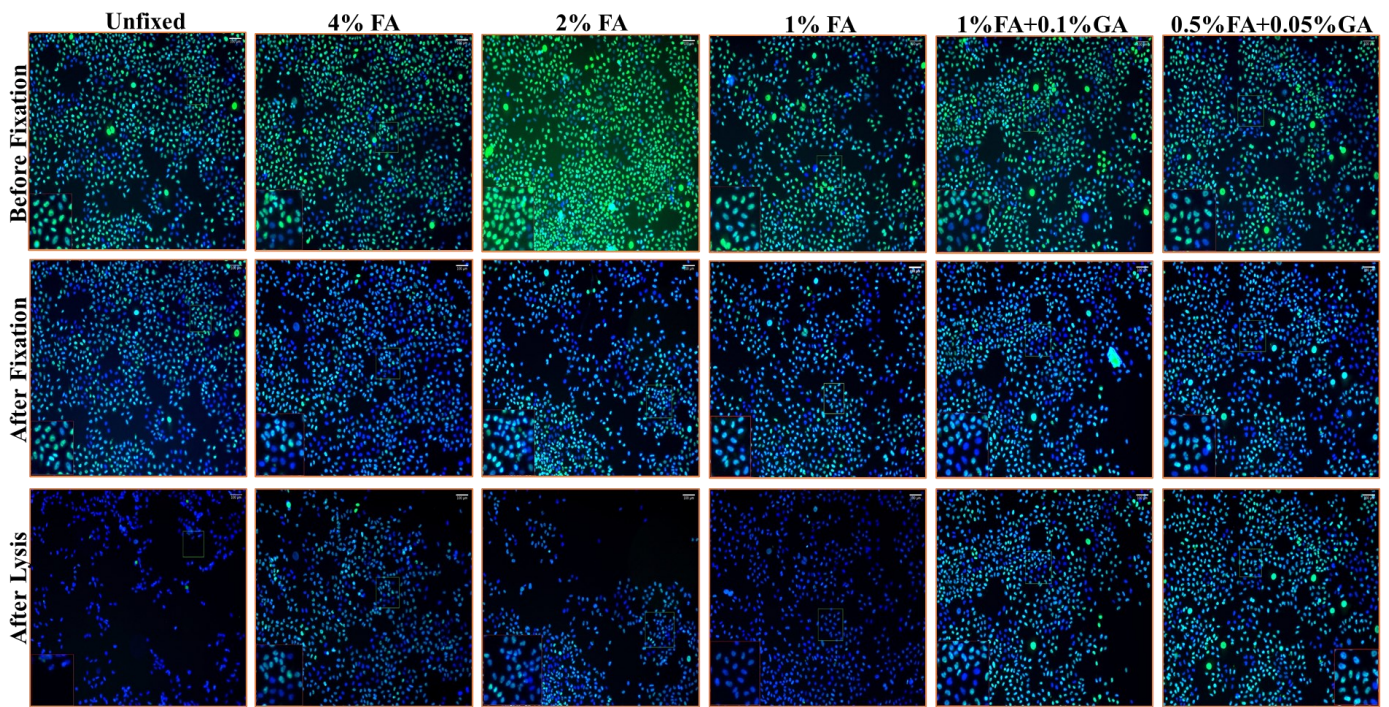


FIGURE 13. HIGH THROUGHPUT IMAGING OF FUS FIXATION WITH DIFFERENT CONCENTRATIONS OF FA AND COMBINATION OF FA AND GA: HeLa GFP-FUS cells were stained with Hoechst and then fixed for 1 minute with different fixatives. After a quick wash with TBS, the cells were lysed for 3 minutes in lysed in NP40+SDS, replaced with TBS and images were collected from 10 x objective. Representative image of live cell shown on the left. Images before fixation, after fixation and Post lysis images of (unfixed), (4%FA), (2%FA), (1%FA), (1%FA+0.1%GA), (0.5%FA+0.05%GA) fixations are shown on the right side.

FRAP ANALYSIS ON CROSSLINKING OF NUCLEAR FUS

Based on the results from high-content screening, FRAP was performed to monitor the immobilization of GFP-FUS using 4 % FA and FA+GA 1 minute fixation. To do this, we followed the same protocol as for GFP-G3BP1. During the 6.4 minutes observation, 490 frames of images with 20 prebleach and 470 post bleach images were obtained to calculate the recovery time of fluorescence after bleaching with bleaching ROI of 3 μm diameter as used for GFP-G3BP1. Live HeLa GFP-FUS cells were used as positive control for fluorescence recovery after bleaching. The fixatives tested were 4 % FA, 0.1 % GA alone and (0.5%FA+0.01%GA) within the 1-minute timeframe. In contrast to GFP-G3BP1, after photobleaching, GFP-FUS fluorescence recovery is significantly slower with 4 % FA fixation and the fluorescence recovered from the initial frame was 27.49 %. Further, (0.5%FA+0.1% GA) and 0.1 % GA showed insignificant recovery (FIGURE 14 PANEL A). Data analysis also showed their recovery curve overlapped indicating that both combination and GA alone were equally efficient in fixing cells with only 19.7 % and 18.8 % respective recovery percentage relative to initial fluorescence (FIGURE 14 PANEL B). Furthermore, the mobile fraction

estimated in the cells fixed with these fixatives were significantly lower with only 0.06 and 0.05 respectively (FIGURE 14 PANEL C). All the three conditions showed significantly more efficient fixation with respect to cytosolic-marker proteins as also assessed with the high throughput imaging results. From the above results, we can conclude that using the same fixation-conditions, nuclear-proteins behave distinctly from cytosolic proteins being more prone to form crosslinked immobile complexes.

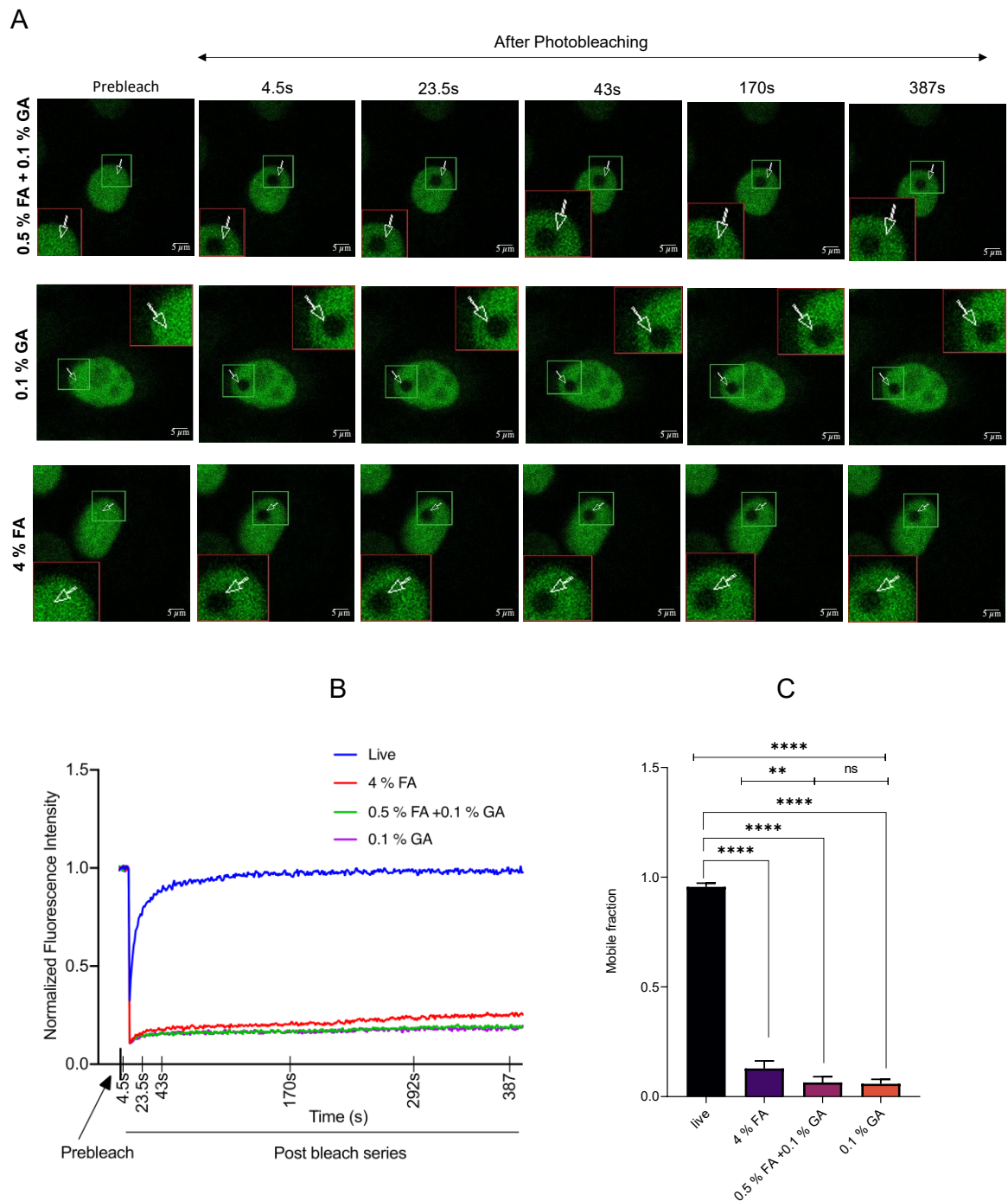


FIGURE 14. FRAP ANALYSIS TO VALIDATE THE CROSSLINKING EFFICIENCY OF THE FIXATIVES FOR CYTOPLASMIC GFP-G3BP1: **PANEL A**-Representative images of HeLa GFP-FUS in the order of first prebleach image, and five images at indicated time points after photobleaching (post bleach 1 t1/200 1-4.5 s, postbleach 1 t100/200-23.5 s, postbleach 1 t200/200-43s, postbleach 2 t125/250-170s, postbleach 3 t20/20-387s). White arrows indicate the ROIs. Scale bar is 5 μ m. **PANEL B**- The graph shows the normalized fluorescence intensity against time after fixation and in live cells. The intervals marked on the x axis are relative to the images presented above. **PANEL C**-The mobile fraction present in each fixation and living cells estimated from individual the curve fits (live, n=5; fixed samples, n=5 each). Data are mean \pm SEM and statistical significance was assessed by Ordinary one-way ANOVA test.

BIOCHEMICAL EXTRACTION & SOLUBILIZATION FOR NUCLEAR LOCALIZED PROTEINS

In order to investigate if the conditions of fixation and lysis could be further used in nuclear RNP immunoprecipitation, HeLa GFP-FUS cells were fixed with increasing concentrations of FA (4, 2, 1 % FA) and combination of FA+GA (0.5%FA+0.1%GA) and (0.5%FA+0.05 %GA) and lysed in NP40+SDS lysis buffer followed by sonication and centrifugation. The lysates were analyzed by SDS PAGE and Western blot. Uncross linked cells (FIGURE 15 PANEL A) showed abundant recovery of GFP-FUS monomers. A decrease in the monomer band of GFP-FUS can be noticed with increasing concentrations of FA and/or GA alone or combination with FA while no crosslinked products are visible in the western blot analysis. Altogether the data presented showed that the lysis/solubilization conditions used do not recover the crosslinked products of GFP-FUS in a soluble form, possibly similarly lost in the pellet fraction as previously seen for p53.

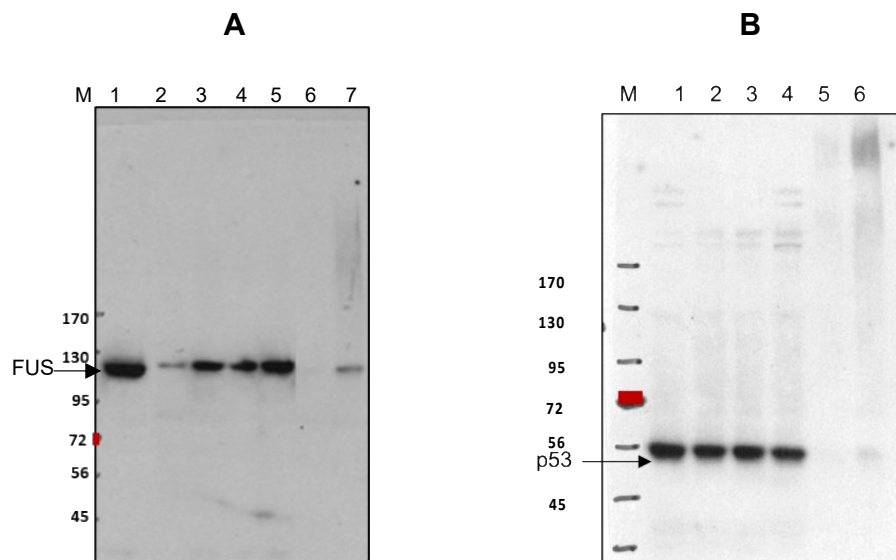


FIGURE 15. SDS-PAGE-Western Blot analysis to check for crosslinked complexes of nuclear targets: HeLa-GFP FUS cells were crosslinked for one minute with different concentrations of FA and combinations of FA and GA, washed quickly with TBS and lysed in NP40/SDS buffer followed by sonication and centrifugation. Clarified lysates were prepared boiling with 2x Laemmli buffer and loaded to 12% SDS PAGE for Western Blot and probed with anti-GFP and anti-p53. **PANEL A**) shows Western blot of FUS: M-Marker; **Lane**

1)Uncrosslinked cell lysate; Lane 2)(8%FA); Lane 3)(4%FA); Lane 4)(2%FA); Lane 5)(1%FA); Lane 6)(0.5%FA+0.1%GA); Lane 7)(0.5%FA+0.05%GA). **PANEL B** shows Western blot of p53: M-Marker; Lane 1) Uncrosslinked cell extract; Lane 2) (4%)FA; Lane 3)(2%FA); Lane 4)(1%FA); Lane 5)(0.5%FA+0.1%GA); Lane 6)(0.5%FA+0.05%GA).

The decreasing monomer species of GFP-FUS with increasing concentration of FA and/or GA indicates effective crosslinking, however no crosslinked products were directly observed as higher molecular weight smears. Similarly, when checked for p53 from the same lysates, no crosslinked products could be shown (FIGURE 15 PANEL B). Lysis in NP40/SDS did not recover the crosslinked products of GFP-FUS or p53 in soluble forms. It was therefore evident that nuclear proteins behave quite differently from cytosolic proteins being more prone to forming higher-order complexes that fail to be solubilized. Since only 'soluble' complexes, that is not precipitated by centrifugation at 13000 x g RCF, are amenable to further biochemical analysis by immuno-isolation, additional or alternative approaches were required to improve extraction from cells crosslinked with the optimized fixative conditions working for cytosolic proteins.

BIOCHEMICAL FRACTIONATION OF CROSSLINKED COMPLEXES

We firstly assumed that crosslinked complexes can be fractionated differentially by the use of ion-exchange chromatography using magnetic beads as matrix, also in combination with Polyethylene Glycol (PEG) and NaCl to force interactions. We used lysates prepared from UV and (0.5 %FA+0.05%GA) fixed HCT-116 stably expressing FLAG-YAP1, by lysis followed by sonication and centrifugation as mentioned before. At first, the lysates were incubated with carboxy-coated magnetic beads (COOH-Beads) for 5 minutes and then the beads were separated from the unbound supernatant. The obtained supernatant was then mixed with 8 % PEG and 0.4 M NaCl final concentrations along with fresh COOH-Beads and incubated for 5 minutes followed by separation of beads and the supernatant. We then analyzed both the supernatants and the material attached to the beads after elution in Laemmli-buffer followed by Western blot analysis shows that histone proteins are mainly detected in the beads from the first step, after addition of PEG and NaCl to the first supernatant while most of YAP1 and its crosslinked complexes were found in the beads (FIGURE 16). Importantly, in the case of FA+GA crosslinked cell lysates, the high molecular weight complexes were mostly enriched in the second step of binding.

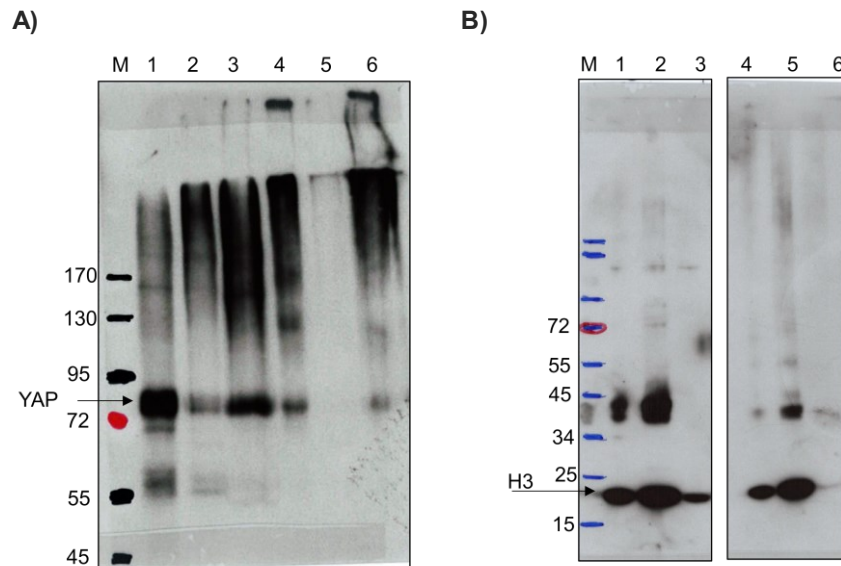


FIGURE 16. FRACTIONATION OF CROSSLINKED COMPLEXES WITH COOH-BEADS: Western blot for YAP1 and Histones. Differential binding of complexes was carried out with lysates prepared from HCT-116 cells stably expressing YAP1. Cells were crosslinked, lysed in DDM/SDS buffer followed sonication and centrifugation. The lysates were fractionated using Carboxy beads by consequent binding and elution. **PANEL A:** The lysates and beads that bound were mixed with 2x Laemmli buffer, boiled and loaded to 12% SDS PAGE for Western Blot. and probed with anti-YAP. The samples were loaded in the following order: **M)** Protein marker; **Lane 1)** UV-crosslinked cell lysate; **Lane 2)** UV crosslinked- Beads without PEG/NaCl; **Lane 3)** UV crosslinked-beads after addition of PEG/NaCl; **Lane 4)** (0.5%FA+0.05%GA) crosslinked cell lysate; **Lane 5)** (0.5%FA+0.05%GA) crosslinked- Beads without PEG/NaCl; **Lane 6)** (0.5%FA+0.05%GA) crosslinked- beads after addition of PEG/NaCl. **PANEL B:** The lysates and beads that bound were mixed with 2x Laemmli buffer, boiled and loaded to 10% SDS PAGE for Western Blot. and probed with anti-H3. The samples were loaded in the following order: M) Protein marker; **Lane 1)** UV-crosslinked cell lysate; **Lane 2)** UV crosslinked- Beads without PEG/NaCl; **Lane 3)** UV crosslinked-beads after addition of PEG/NaCl; **Lane 4)** (0.5%FA+0.05%GA) crosslinked cell lysate; **Lane 5)** (0.5%FA+0.05%GA) crosslinked-Beads without PEG/NaCl; **Lane 6)** (0.5%FA+0.05%GA) crosslinked- beads after addition of PEG/NaCl.

We then checked a similar protocol for differential purification of crosslinked-protein complexes with positively charged beads containing amino group (DEAE-beads). Both YAP1 and histones were found to bind DEAE beads in the absence of PEG and NaCl (FIGURE 17). This strongly indicated the possibility of using the charged beads for fractionating complexes and/or clarifying the lysates from non-target proteins or complexes.

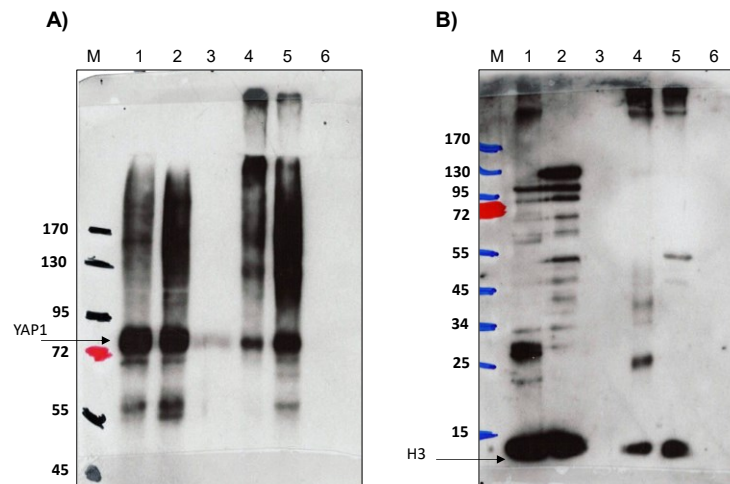


FIGURE 17. FRACTIONATION OF CROSSLINKED COMPLEXES WITH DEAE BEADS BY WESTERN BLOT FOR YAP1 AND HISTONES: Differential binding of complexes was carried out with lysates prepared from HCT-116 cells stably expressing YAP1. Cells were crosslinked, lysed in DDM/SDS buffer followed sonication and centrifugation. The lysates were fractionated using DEAE beads by consequent binding and elution. **PANEL A: The lysates and beads that bound were mixed with 2x Laemmli buffer, boiled and loaded to 12% SDS PAGE for Western Blot and probed with anti-YAP.** The samples were loaded in the following order: **M) Protein marker; Lane 1) UV-crosslinked cell lysate; Lane 2) UV crosslinked- Beads without PEG/NaCl; Lane 3) UV crosslinked-beads after addition of PEG/NaCl; 4) (0.5%FA+0.05%GA) crosslinked cell lysate; Lane 5)(0.5%FA+0.05%GA)crosslinked-Beads without PEG/NaCl; Lane 6) (0.5%FA+0.05%GA) crosslinked- beads after addition of PEG/NaCl.** **PANEL B: The lysates and beads that bound were mixed with Laemmli buffer, boiled and loaded to 12% SDS PAGE for Western Blot and probed with anti-H3.** The samples were loaded in the following order: **M) Protein marker; Lane 1) UV-crosslinked cell lysate; Lane 2) UV crosslinked- Beads without PEG/NaCl; Lane 3) UV crosslinked-beads after addition of PEG/NaCl; Lane 4) (0.5%FA+0.05%GA) crosslinked cell lysate; Lane 5) (0.5%FA+0.05%GA) crosslinked-Beads without PEG/NaCl; Lane 6) (0.5%FA+0.05%GA) crosslinked- beads after addition of PEG/NaCl**

A UNIFIED PROTOCOL FOR CYTOSOLIC AND NUCLEAR CROSSLINKED-COMPLEXES BY MAGNETIC BEADS IMMOBILIZATION AND TREATMENT FOR DIFFERENTIAL DISSOLUTION

Based on the observations obtained from differential binding of complexes to carboxy-coated magnetic beads, an idea emerged to test if GA crosslinked products could be directly captured from the cells. To do this, U2OS GFP-G3BP1 cells were fixed with (0.05%GA), (0.1%GA) and combination (0.5%FA+0.05%GA). Uncrosslinked cells were used as control. To extract cellular components, we omitted SDS from the NP40 based buffer (50 mM Tris, pH 8, 100 mM NaCl, 1 % NP40 and 2 mM EDTA). Just after the addition of the above specified lysis-buffer directly to the culture plate that is previously fixed and washed with TBS, 30 μ l carboxy-conjugated magnetic beads from the original stock of suspension (prewashed with TBS) was added to the plate. This allowed chemical lysis of the cells and concurrent binding of the released complexes to the

negatively charged carboxy beads. This protocol does not involve harsh mechanical treatments like sonication except for 5-10 minutes of mixing of the beads. The first step produced two fractions: the supernatant containing unbound material separated by magnetic support and the beads containing bound material. The supernatant was completely soluble and did not form any visible pellet after centrifugation at 13000 x g RCF. In order to identify what was bound to the beads, they were eluted in 2x Laemmli buffer by boiling for 5 minutes. The supernatant was also prepared with Laemmli buffer for analysis. The results showed that higher amount of G3BP1 was present in the supernatant from uncrosslinked cells and decreased with increasing concentration of fixatives. At difference with the uncrosslinked control lysate where GFP-G3BP1 remained in the supernatant, most of the crosslinked G3BP1-products were distinctly found in the beads-bound material (FIGURE 18 A)

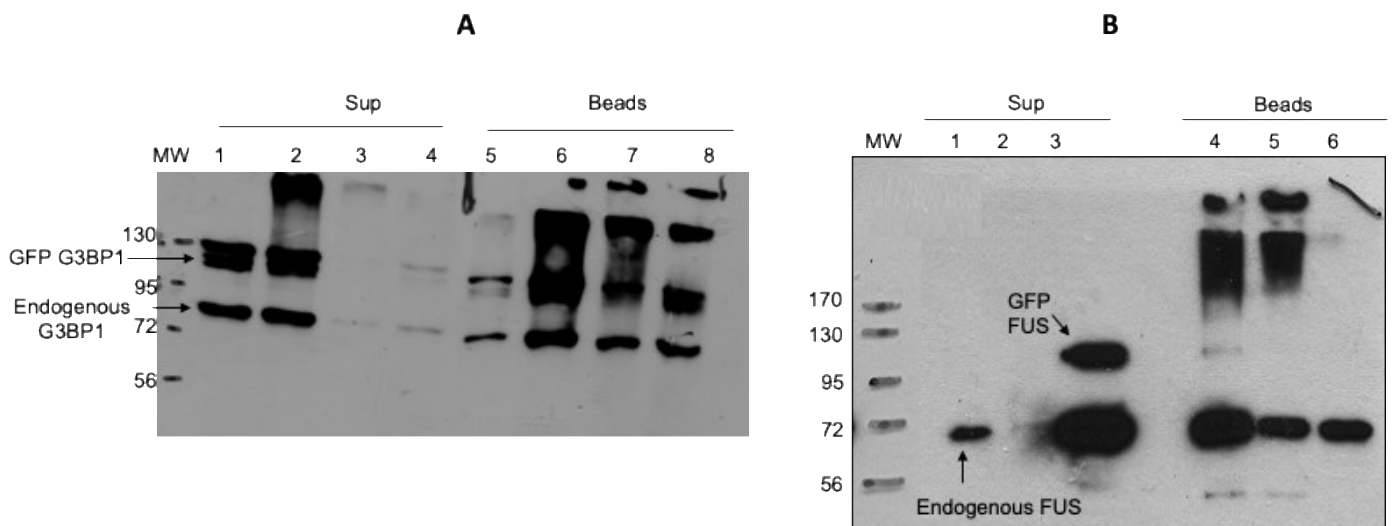


FIGURE 18. BEAD LYSIS AND CAPTURE OF CROSSLINKED COMPLEXES: PANEL A: U2OS-GFP-G3BP1 cells (with or without crosslinking) lysed with COOH-beads. The unbound material was separated with the help of magnetic support and mixed with Laemmli buffer, boiled for 5 minutes for SDS-PAGE/Western Blot. The bound material on the beads were eluted by boiling in Laemmli buffer. Comparable amounts of supernatants (sup) and eluates from beads (beads) were analysed by 12 % SDS-PAGE/Western blot for anti G3BP1. The upper band corresponds to GFP-G3BP1, while the lower band corresponds to Endogenous G3BP1. The samples were loaded in the following order: **MW** represent molecular weight marker; **Lane 1)** (uncrosslinked sup); **Lane 2)**(0.05%GA-sup); **Lane 3)**(0.1%GA-sup); **Lane 4)**(0.5%FA+0.05%GA-sup); **Lane 5)** eluted material from (uncrosslinked-beads); **Lane 6)** eluted material from (0.05%GA); **Lane 7)** eluted material from (0.1%GA); **Lane 8)** eluted material from (0.5%FA+0.05%GA). **PANEL B:** HeLa-GFP-FUS cells (with or without crosslinking) lysed with the addition of COOH-beads. The unbound material (sup) was separated with the help of magnetic support and mixed with Laemmli buffer, boiled for 5 minutes for SDS-PAGE/Western Blot. The bound material on the beads were eluted by boiling in 2x Laemmli buffer. Comparable amounts of supernatants (sup) and eluates from beads (beads) were analysed by 12 % SDS-PAGE/Western blot for anti FUS. Arrows indicate bands of G3BP1. The samples were loaded in the following order: **MW** represent molecular weight marker; **Lane 1)**

(0.5%FA+0.05%GA-sup); **Lane 2**(0.1%GA-sup); **Lane 3** (uncrosslinked-sup); **Lane 4** eluted material from (0.5%FA+0.05%GA); **Lane 5** eluted material from (0.1%GA); **Lane 6** eluted material from (uncrosslinked)

We then tested the protocol for FUS specific complexes for which HeLa GFP-FUS cells were fixed and lysed under same conditions used for U2OS-GFP-G3BP1. Remarkably similar to GFP-G3BP1, crosslinked products of FUS of fixed cells were also seen only in the bound material recovered from beads while the uncrosslinked control GFP-FUS remained in the supernatant. (FIGURE 18 B). The complexes bound to the beads have to be eluted from the beads conserving their ability to interact with the antibodies used for the subsequent specific immunoprecipitation.

To do this, firstly, we tried elution with high salt at pH 8. (FIGURE 19). When checked by Western Blot, G3BP1 crosslinked complexes were found to elute with high salt, however most of them were still found in harsh and alkaline elution (100 mM NaOH) which was due to difference in the charge of the proteins that were bound to the beads.

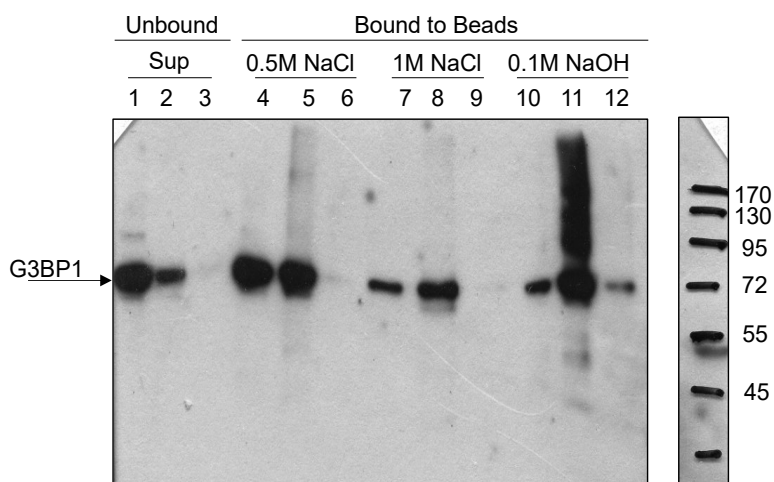


FIGURE 19. ALKALINE ELUTION OF CROSSLINKED COMPLEXES BOUND TO COOH BEADS: HeLa-GFP-FUS cells (with/without crosslinking) lysed with the addition of COOH-beads. The unbound material (mentioned as sup) was separated with the help of magnetic support and mixed with Laemmli buffer, boiled for 5 minutes for SDS-PAGE/Western Blot. Firstly, the beads were eluted with 0.5M NaCl, followed by 1 M NaCl, then by 0.1 M NaOH. The samples were mixed with Laemmli buffer, boiled for 5 minutes and analysed by 12 % SDS-PAGE/Western blot for anti G3BP1. The following lanes represent unbound supernatants: **Lane 1**(uncrosslinked-sup); **Lane 2**(0.1%GA-sup); **Lane 3**(0.5%FA+0.1%GA-sup); The following lanes represent elution with 0.5M NaCl: **Lane 4**(uncrosslinked-0.5M NaCl); **Lane 5**(0.1%GA-0.5M NaCl); **Lane 6**(0.5%FA+0.1%GA-0.5M NaCl); The following lanes represent elution with 1M NaCl: **Lane 7**(uncrosslinked cells-1M NaCl); **Lane 8**(0.1%GA-1M NaCl); **Lane 9**(0.5%FA+0.1%GA-1M NaCl); The following lanes represent elution with 0.1 M NaOH: **Lane 10**(uncrosslinked-0.1M NaOH); **Lane 11**(0.1%GA-0.1M NaOH); **Lane 12**(0.5%FA+0.1%GA-0.1M NaOH).

Next, in order to improve the elution of crosslinked complexes, (0.1%GA) crosslinked HeLa cells were lysed using COOH-beads under same conditions and the beads were incubated with a buffer containing 50 mM

Ammonium sulphate ((NH₄)₂SO₄) and 0.5 % SDS, in 15 mM Tris-Cl pH 8 for 10 minutes in the cold. This was repeated again to recover any complexes weakly bound to the beads. After the previous elution steps, 0.1 M sodium hydroxide was added, incubated for 5 minutes and the elution was collected. Then, the beads were collected and finally mixed with 2x Laemmli buffer and boiled for 5 minutes to recover the remaining bound material. In the case of G3BP1, first elution with (NH₄)₂SO₄/SDS allowed most of the crosslinked products to be elute (FIGURE 20 PANEL A). Only a small fraction of complexes was recovered in the following elution steps. However, when the same samples were probed for FUS (FIGURE 20 PANEL B) and YAP1 (FIGURE 20 PANEL C), elution was not complete with NH₄SO₄/SDS. As opposed to G3BP1, small fraction of specific complexes was recovered from the beads at first elution while most of them were eluted by boiling in 2x Laemmli buffer. Therefore, to be able to elute FUS and YAP specific complexes better, we plan to resuspend the beads in (50mM (NH₄)₂SO₄+0.5%SDS) and heat of 80°C or to find more efficient competing anions to dislodge the complexes from the Carboxy-beads.

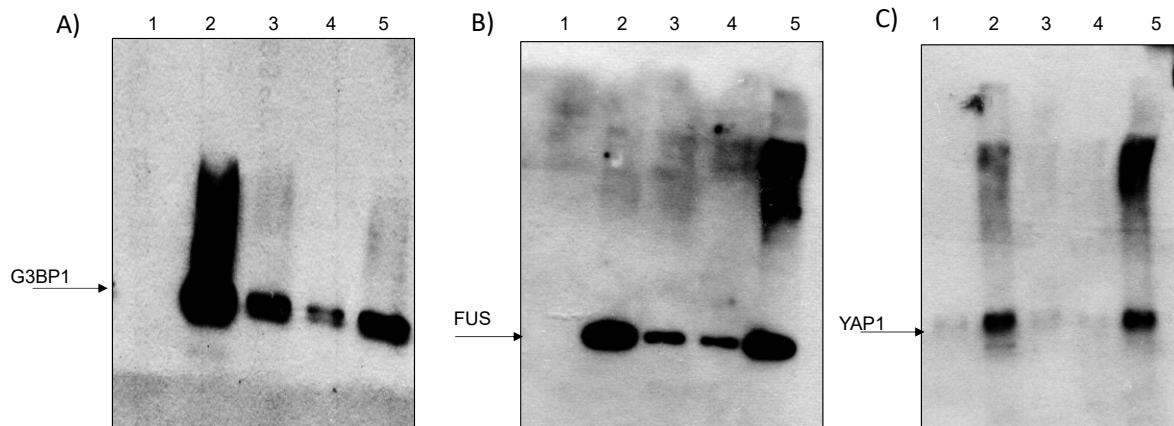



FIGURE 20. ELUTION OF CROSSLINKED COMPLEXES WITH AMMONIUM SULPHATE AND SDS: HeLa Cells were crosslinked with 0.1%GA and lysed with the addition of COOH-beads. The unbound material (mentioned as ‘sup’) was separated with the help of magnetic support and mixed with Laemmli buffer, boiled for 5 minutes for SDS-PAGE/Western Blot. Firstly, the beads were eluted with (NH₄)₂SO₄/SDS buffer, followed by repeated elution with (NH₄)₂SO₄/SDS, followed by 0.1M NaOH. Finally, the beads were boiled in 2x Laemmli buffer for 5 minutes. All other samples were also mixed with Laemmli buffer, boiled for 5 minutes and analysed by 12 % SDS-PAGE/Western blot. **PANEL A: Western blot probed with anti-G3BP1.** The samples were loaded in the following order: **Lane 1)** Unbound Supernatant; **Lane 2)** first elution in (NH₄)₂SO₄; **Lane 3)** second elution in (NH₄)₂SO₄; **Lane 4)** Elution in 0.1M NaOH; **Lane 5)** Elution in 2x Laemmli. **PANEL B): Western blot probed with anti-FUS.** The samples were loaded in the following order: **Lane 1)** Unbound Supernatant; **Lane 2)** first elution by (NH₄)₂SO₄; **Lane 3)** second elution by (NH₄)₂SO₄; **Lane 4)**0.1M NaOH; **Lane 5)** Elution in 2x Laemmli. **PANEL C): Western blot probed with anti-YAP1.** The samples were loaded in the following order: **Lane 1)** Unbound Supernatant; **Lane 2)** first elution by (NH₄)₂SO₄; **Lane 3)** second elution by (NH₄)₂SO₄; **Lane 4)**0.1M NaOH; **Lane 5)** Elution in 2x Laemmli



As we proceed, we are customizing every step to precisely characterize transient interactions occurring in macromolecular condensates. Further work will concentrate on validating the viability of eluted complexes for specific immunoprecipitation. Glutaraldehyde might cause masking of epitope of the protein in the meshwork of crosslinking (Paavilainen *et al.*, 2010). This will be strategically solved by antigen retrieval protocol that employs heat at specific pH suitable for the molecule of interest (Bogen, Vani and Sompuram, 2009). After antigen retrieval, the specific complexes will be immunoprecipitated.

Recent studies showed that hyperosmotic stress leads to macromolecular condensates enriched with lncRNA-markers such as NORAD in stress granules and NEAT1 for paraspeckles (Matheny *et al.*, 2020). Thus, to validate the methodology developed, we will analyse the compositional identity of the stress granules and nuclear paraspeckles with G3BP1 and FUS as their protein handles respectively by RT-PCR with respect to control depleted mRNAs such as GAPDH and other non-specific RNAs.

PRIMARY SCREENING OF FIXATIVES FOR OPTIMIZING SHORT FIXATION PROTOCOL

In our attempts to choose the best protocol for snap-shot crosslinking based on formaldehyde, a number of reagents were tested by SDS PAGE and Western blot as well as high throughput imaging. Initially, we hypothesized that certain compounds could act as catalyst to increase of the efficiency of fixatives thus allowing a decrease in the time of fixation. To investigate this, we tested different amines dimethylhexylamine (DMHA) and dimethylcyclohexylamine (DMCHA), Quinuclidine (QNU), and N,N-Dimethylmethyleiminium chloride (NNDMM) by high throughput imaging in combination with 0.5 % FA. Their fixation efficiencies are not appreciable as there was a total loss of GFP signals in the cells (FIGURE 21).

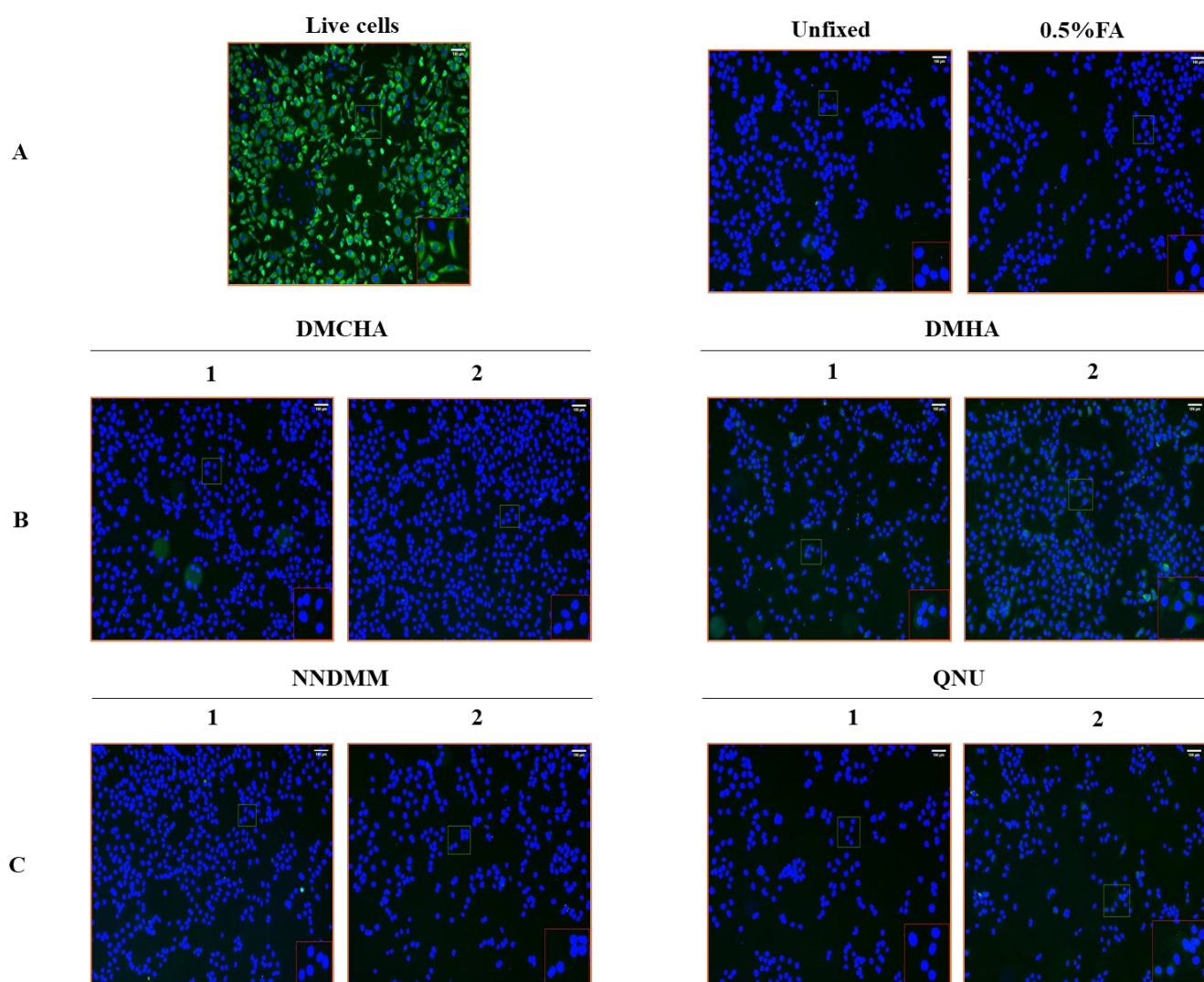


FIGURE 21. High Throughput Imaging to identify catalysts to improve FA crosslinking: Representative images shown here were acquired post lysis treatment with DDM/SDS buffer, with U2OS GFP-G3BP1 cells previously fixed and washed with specific crosslinking solutions. **PANEL(A)** Live cells imaged after Hoechst staining (left); Unfixed cells after lysis (middle); 0.5%FA (right) **PANEL (B)** shows cells after lysis. **Dimethyl-cyclohexylamine (DMCHA) as catalyst:** 1- 0.5%FA+25 mM-DMCHA; 2- 0.5%FA+50 mM DMCHA **PANEL(C) Dimethyl Hexylamine (DMHA) as catalyst:** 1-0.5%FA+25 mM-DMHA; 2-0.5%FA+50 mM-DMHA. **PANEL(C)** shows cells after lysis. **N,N-Dimethylmethyleiminium chloride (NNDMM) as catalyst:** 1- 0.5%FA+0.1 M NNDMM; 2- 0.5%FA+0.2 M NNDMM; **Quinoline (QNU):**1-0.5%FA+25 mM QNU; 2- 0.5%FA+50 mM QNU, scale bar is 100 μ m

Using HCT-116 FLAG-YAP cells as model system, some more conditions were evaluated biochemically by preparing the lysates as before and analysis by Western blot for YAP1. 0.5 % FA combined with cyclohexylamine showed improved crosslinking with higher molecular weight smears. In consistent to our previous observation, 0.05 % GA in combination with 0.5 % FA showed remarkable crosslinking of proteins. Other compounds like phenyl glyoxal, 1-ethyl-3-(3-dimethylaminopropyl) carbodiimide hydrochloride (EDC), Boric acid, and PA were not effective, hence were ruled out of our choices for further analysis (FIGURE 22 A). However, with the positive crosslinking ability seen with cyclohexylamine, we hypothesized tertiary amine like dimethylcyclohexylamine could be more effective catalysts, hence tested at different concentrations in combination with 0.5 % FA.

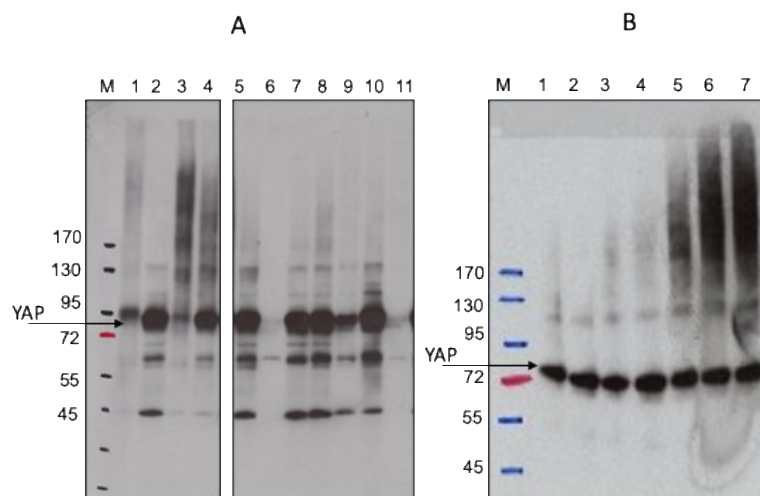



FIGURE 22. SCREENING OF DIFFERENT CROSSLINKING AGENTS BY WESTERN BLOT ANALYSIS FOR YAP1 CROSSLINKED LYSATES FROM HCT-116 FLAG-YAP1 CELLS: **PANEL A)** Western Blot for screening of different fixatives probed for YAP. M-protein marker; **Lane 1)** UV; **Lane 2)**(0.5%FA); **Lane 3)**(0.5%FA+0.05%GA); **Lane 4)**(75mM CHA+0.5%FA); **Lane 5)**(75mM Boric acid+0.5%FA); **Lane 6)**(200 mM EDC+75 mM CHA); **Lane 7)**(200 mM EDC+MES pH 6.5); **Lane 8)**(200 mM EDC+MES+PA); **Lane 9)**(200 mM Phenyl glyoxal+MES); **Lane 10)**(200 mM Phenyl glyoxal+MES+PA); **Lane 11)**(200 mM Phenyl glyoxal+75 mM CHA). **PANEL B)** shows Western Blot for the titration of DMCHA probed for for YAP. M protein marker; **Lane 1)**UV; **Lane 2)**(0.5%FA); **Lane 3)**(0.5%FA+5 mM DMCHA); **Lane 4)**(0.5%FA+10 mM DMCHA); **Lane 5)**(0.5%FA+25 mM DMCHA); **Lane 6)** (0.5%FA+50 mM DMCHA); **Lane 7)**(0.5%FA+75 mM DMCHA)



From the Western blot for YAP, it was seen that 0.5 % FA formed YAP1 specific higher molecular weight products in the presence of amine, and with increasing concentrations of DMCHA, the band density of crosslinked products also increased. In comparison, the 0.5 % FA without amine showed no crosslinked products in their lysates. Despite this, uncrosslinked monomer species did not decrease with the increased crosslinking products unlike with GA based fixatives (FIGURE 22 B). Therefore, use of amines was ruled out.

Ultimately, our attempts to find the best fixative suitable for rapid crosslinking protocol indicated that GA alone or in combination with FA to be the most appropriate fixative to achieve highly effective crosslinking in a minute or less.



DISCUSSIONS

Biocondensates are dynamic microcompartments with changing compositions of proteins, RNA, and other molecules. We hypothesized that navigation of transcription factor (like p53) or co regulators (like YAP1) between intracellular structures may be facilitated by the formation of Ribonucleoprotein (RNP) condensates and subsequent-guided interactions within a 'liquid-informational-flow'. The high dynamics of RNA-protein and RNA-condensate interactions makes it very complicated to characterize the compositional/RNA-identity of such transient structures with available methodologies (Colantoni *et al.*, 2020).

In order to follow the dynamic changes in RNP condensates and more specifically in the RNA-compositional identities, a rapid and efficient crosslinking protocol is a prime requirement. Classical methods as used for ChIP follow crosslinking for 10 minutes or more which might miss the interactions that occurs only for seconds or minutes (Schmiedeberg *et al.*, 2009). On the contrary UV-based CLIP assays are limited to the analysis of next-near-neighbour loosing global compositional identities. Our preliminary results with 0.1 % formaldehyde fixation for 10 minutes were unsatisfactory due to a lot of non-specific RNAs identified from YAP1-IPs. Therefore, it is important to ensure that short lived protein -RNA associations are rapidly crosslinked and preserved. Optimization is essential for obtaining their snap-shot and subsequent biochemical separation maintaining their global composition. To address this, we tested different crosslinking agents and catalytic agents by high content imaging. Our high content imaging method to screen for fixatives was a two-dimensional approach in which the fixatives were tested against lysed cells, thus allowing us to achieve a balance between the crosslinking and extraction of the crosslinked complexes (Zeng, Yang and Huang, 2013). The primary aim was to achieve maximum crosslinking in one minute or less. One of the major components of stress granules (SGs) and cytoplasmic localized protein GFP-tagged G3BP1 was used as marker model system for further optimization experiments (Deniz, 2020). We screened different compounds including formaldehyde, glutaraldehyde, amines as catalysts, transporters and blockers. Among all, glutaraldehyde showed significant crosslinking abilities by achieving higher degree of fixation in one minute at—a concentration down to 0.05 % corresponding to 5mM. Meanwhile, formaldehyde was required at a concentration of >40 times more than glutaraldehyde to achieve levels of fixation comparable to 0.05% GA. Inspired by Karnovsky-type fixative, we combined small concentration of formaldehyde with glutaraldehyde to allow fast and mild extracellular-plasma membrane fixation by the slowly diffusing formaldehyde allowing for fast diffusion of glutaraldehyde and its concomitant intracellular fixation (Karnovsky M J, 1974). Evidently, the combination fixative showed better fixation of cytoplasmic GFP-G3BP1 (Huebinger *et al.*, 2018). We highlighted three conditions of crosslinking that allowed the cells to achieve a balanced fixation and lysis of cytoplasmic components from High content imaging. The shortlisted candidate fixatives were re-evaluated for immobilization efficiency in real time by Fluorescence Recovery After Photobleaching (FRAP). FRAP analysis showed that 4 % FA steadily recovered fluorescence over time thus indicating its less effective

for fixing cytoplasmic G3BP1. On the other hand, combinations of FA and GA crosslinked more proficiently than FA or GA alone. Altogether, high content imaging and FRAP analyses on GFP-G3BP1 revealed that GA based fixation could be useful to achieve maximum crosslinking of molecules within cytoplasm within one minute exposure to the fixative. Based on these conditions, we carried out biochemical analysis cells fixed by different concentrations of FA and FA+GA combinations. The crosslinked products specific to G3BP1 and YAP1 were extracted effectively in DDM+SDS lysis buffer. Moreover, immunoprecipitation performed to understand recoverability of specific extracted complexes for further analysis. This was essential to check if crosslinking protocol affects immune capture of the specific proteins. It was of interest to see the enrichment of crosslinked products both of G3BP1 and YAP1 in the eluates.

When we attempted to validate the same protocol for p53, there was poor extractability of crosslinked products. We re-assessed the crosslinking agents and extraction protocol with the help of a nuclear marker GFP-FUS, which is known to be involved in the formation of paraspeckles, among its numerous nucleosome localizations (Hennig *et al.*, 2015). Therefore, we tested different concentrations of formaldehyde and combinations of FA and GA. We chose to perform formaldehyde titration in order to identify the least concentration of formaldehyde that can achieve maximum crosslinking in one minute. Given that NP40 is more efficient in dissolving nuclear membrane (Holden and Horton, 2009) as compared to DDM, we performed the High content imaging coupled with NP40/SDS buffer for lysis. Similar to G3BP1, 4 % FA was required for achieving reasonable degree of crosslinking in GFP-FUS. However, combination of FA and GA were more efficient in preserving the cellular integrity as indicated by the GFP-FUS containing nuclei. In agreement with high throughput analysis, FRAP showed that 4 % FA was far better in crosslinking nuclei than cytoplasm. Of note, 0.1 % GA and 0.5 % FA+0.1 % GA were more effective solutions for rapid crosslinking of nuclear protein.

Taken together all the above results, biochemical experiments were performed to check the extractability of nuclear proteins FUS and p53 using the optimized fixation protocol. Both nuclear proteins showed a poor recovery of crosslinked products that were lost in insoluble pellet. Increasing sonication strength and time to extract nuclear proteins did not significantly increase the solubility of crosslinked complexes. That the entire workflow is in need of an alternative approach was in fact clear right from the beginning. After introducing the snap-shot crosslinking, the next problem encountered was formation of insoluble pellet as referred to nuclear proteins that formed after conventional lysis processes (Kustatscher *et al.*, 2015). Mechanical treatment like sonication or homogenization to lyse the cells is typically used. However, mechanical processes are highly variable and are not scalable precisely. So, we were in search for a more rational and scalable

approach which depends on chemical aspects. Since sonication regimes are quite variable and even more from lab-to-lab, we searched for more scalable alternatives.

In a parallel line of investigations, we tried to fractionate the complexes using ion-exchange-chromatography by the use of charged magnetic beads. It was of interest to see differential binding proteins and their complexes to the beads (Kim *et al.*, 2020). YAP1 and its crosslinked complexes bound to the negatively charged beads in the presence of crowding agent PEG and NaCl, whereas histones bound without PEG and NaCl. We similarly analysed positively charged tertiary amine (DEAE) beads, showing that YAP1 and its complexes bound to the beads in the absence of any crowding agent. Surprisingly, Histones were also found to bind the positively charged beads under the same conditions. These results indicated to us that charged-magnetic-beads can be used for differential capture of complexes.

Glutaraldehyde crosslinking of proteins forms positively charged pyridine polymers rapidly (Johnson, 1993). Perhaps, formation of positively charged product might be useful for direct capture of crosslinked products by negatively charged magnetic beads. Thus, we combined the process of lysis and capture of complexes in a single step. Here, carboxy-beads added together with the detergent could act as a mimic of anionic detergents for simultaneous capture of extracted complexes. Biochemical analysis justified hypothesis by showing no binding of uncrosslinked species of GFP-G3BP1 to the beads from unfixed/uncrosslinked cells, whereas beads captured GFP-G3BP1 crosslinked complexes from fixed cells. As there was no insoluble pellet formed from either fraction, problems of balancing crosslinking efficiency and associated protein loss are well addressed by our method (Kast and Klockenbusch, 2010).

As we proceed, we are customizing every step to precisely characterize transient interactions occurring in macromolecular condensates. Further work will concentrate on validating the viability of eluted complexes for specific immunoprecipitation. Glutaraldehyde might cause masking of epitope of the protein in the meshwork of crosslinking. This will be strategically solved by antigen retrieval protocol that employs heat at specific pH suitable for the molecule of interest (Bogen, Vani and Sompuram, 2009). After antigen retrieval, the specific complexes will be immunoprecipitated and analysed for their RNA partners.

In conclusions, we attempted to address the basic problems in the characterization of RNP condensates. The central point of this work was to develop a robust protocol that allows invariable characterization of transient interactions in biomolecular condensates. Our hypothetical models of YAP and p53 associated complexes challenged us with consecutive problems in identifying their interacting partners. Consequently, we focussed on optimizing the methods with the aid of two marker proteins, G3BP1 and FUS, that are components of stress granules and paraspeckles respectively. In order to rapidly crosslink weak and transient interactions, we

proposed to use glutaraldehyde-based fixatives that can freeze the molecular events in the cell in seconds. However, difference in crosslinking efficiency manifested between cytoplasm and nucleus led to problems in extraction of nuclear proteins, thus required revalidation of crosslinking and lysis process exclusively for nuclear proteins. Our attempts to fractionate the complexes with charged beads exemplified the use of carboxy beads for simultaneous lysis and capture of the crosslinked complexes. This method not only allowed for differential binding of crosslinked complexes and but also high extractability unlike canonical protocols without mechanical disruption. Recent studies showed that hyperosmotic stress leads to macromolecular condensates enriched with lncRNA-markers such as NORAD in stress granules and NEAT1 for paraspeckles (Matheny *et al.*, 2020). Thus, to validate the methodology developed, we will analyse the compositional identity of the stress granules and nuclear paraspeckles with G3BP1 and FUS as their protein handles respectively by RT-PCR with respect to control depleted mRNAs such as GAPDH and other non-specific RNAs.



MATERIAL & METHODS

CELL CULTURE AND MAINTENANCE

U2OS-GFP-G3BP1 was a kind gift from Dr Paul Anderson Harvard Medical School, HeLa BAC540-GFP-FUS was a kind gift from Dr. Simon Alberti Technische Universität Dresden All the cells were cultured and maintained in High Glucose Dulbecco's Modified Eagle Medium (DMEM) with sodium pyruvate and glutamine (Euroclone ECM0728) with 10 % Fetal Bovine Serum (Euroclone ECS0180L). The cells were plated at least 36 hours prior to experiments. For wt-p53 we used the CRISPR-CAS9 engineered HCT-116 p53+/p53-FLAG, which bears the FLAG-tag at the COOH-end, as kindly provided by Dr. Sven Eyckerman, VIB Ghent. We obtained wtYAP1-FLAG by infecting HCT-116 mother-cell line with the retroviral-packaged pBABE-YAP1 N-terminal-FLAG (in collaboration with Prof. Del Sal – LNCIB).

FIXATION

For crosslinking, the media was removed, and cells were washed briefly with 20 mM HEPES, pH 7.4 containing 150 mM NaCl (HBS). In case of UV crosslinking, the cells were exposed to radiation of 2000 mA set on UV strata-linker (Stratagene). It takes approximately 4 minutes to complete. Then the cells were immediately immersed in cold lysis. For chemical fixation, methanol free formaldehyde (Pierce™- 28906), glutaraldehyde (Sigma-Aldrich- G5882), A fresh stock of 4 % FA was prepared in deionized water for the preparation of formaldehyde and formaldehyde-based fixation solutions. Similarly, 2.5 % glutaraldehyde was prepared as a stock for fixation. The cells were fixed with fixative of interest for specified time and the fixatives was removed. Then, the cells were briefly washed with 20 mM Tris, pH 7.8 containing 150 mM NaCl (TBS), since Tris is a primary amine used for quenching the aldehydes. Based on the experiment to proceed, lysis buffer or HBS was added to the cells. Other reagents used for screening were N,N-Dimethylcyclohexylamine, 99% (Sigma-Aldrich, 290629), N,N-Dimethylhexylamine, 99% (Sigma-Aldrich,308102), N,N-cyclohexylamine, 99% (Sigma-Aldrich, C104655), Quinuclidine (Thermo Fisher Scientific, H54498), N,N-Dimethylmethyleiminium chloride (Sigma-Aldrich, 40766).

HIGH THROUGHPUT IMAGING

U2OS GFP-G3BP1 (5×10^3 cells/well) and HeLa GFP-FUS (5×10^3 cells/well) were seeded into CellCarrier-96 Ultra Microplates 36 hours before the experiment. Cells were stained with Hoechst 33342 (Invitrogen™, H3570) at 5000 dilution in HBS for 10 minutes. In the initial setting, cells were imaged at 10 x magnification (Olympus 10x NA 0.95) with a PerkinElmer Operetta High content microscope to check for Hoechst staining. Cells were then washed with HBS and the test concentration of fixative in HBS was added and left for 1 minute at room temperature. Then the fixative was removed, and the cells were briefly rinsed with TBS. When

specified, images were acquired. To the fixed cells, the lysis buffer containing 20 mM Tris, pH 7.8, 150 mM NaCl, 0.6 % Dodecyl Maltoside (DDM) (Cube Biotech), 0.1 % SDS and 2 mM EDTA, or 20 mM Tris, pH 7.8, 150 mM NaCl, 0.6 % NP-40 (IGEPAL CA-63, Sigma), 0.1 % SDS and 2 mM EDTA supplemented with RNase inhibitor (InvitrogenTM-RNaseOUTTM) and protease inhibitor (Sigma-Aldrich, P8340) was added. After 3 minutes, the lysis buffer was removed, and TBS was added to the wells containing cells and final images were collected again. The images with EGFP filter and DAPI filter for GFP were simultaneously acquired and merged with Columbus software.

FLUORESCENT RECOVERY AFTER PHOTBLEACHING (FRAP)

GFP-G3BP1 U2OS cells and GFP-FUS HeLa cells were grown on glass-bottom chambered coverslips (μ -slide 4 well, Ibidi GmbH, Germany) and subjected to FRAP at room temperature. Unfixed living cells were examined as control. Before fixation of each individual well, cells were maintained in HEPES-supplemented medium to stabilize pH at room atmosphere. FRAP measurements were performed on a Leica TCS SP8 confocal microscope (Leica Microsystems GmbH, Mannheim, Germany) using a Plan Achromat 63 \times 1.4 NA oil-immersion objective and the 488 nm line of an Argon ion laser. Images were acquired at 4 Airy Units pinhole aperture, 700 Hz scan speed in bidirectional mode and a 256 \times 256 pixel digital resolution. Twenty pre-bleach images were acquired at minimum laser intensity every 189 milliseconds (ms). Bleaching was performed on a circular spot of 3 μ m diameter. A single high intensity iteration of the 488-nm laser line was used for the bleach pulse, which lasted \sim 160 ms. Two hundred recovery images were then acquired every 189 ms, followed by 250 recovery images at 1-s and 20 images at 5-s intervals using pre-bleach acquisition settings. The mean fluorescence intensities from the photobleached area, the whole cell of U2OS GFP-G3BP1 or nucleus of HeLa GFP-FUS and the background were measured using Fiji (Schindelin *et al.*, 2012) When needed, time series were corrected for xy drift using the Fiji plugin Template Matching and Slice Alignment (<https://sites.google.com/site/qingzongtseng/template-matching-ij-plugin>). Recovery curves were obtained by subtracting background values followed by double normalization, using EasyFRAP-web (Koulouras *et al.*, 2018). The first 10 pre-bleach values were discarded from the analysis. The recovery kinetics shown are averages of normalized curves obtained from multiple individual cells. Mobile fractions were determined in EasyFRAP-web from exponential equations fitted to individual FRAP curves.

CELL DISRUPTION WITH SONICATION

For biochemical analysis, the cells were lysed in lysis-buffer 20 mM Tris, pH 7.8, 150 mM NaCl, 0.6%DDM or 0.6%NP40 with 0.1%SDS. The cells were disrupted by sonication with Branson Sonifier SF150 at 20 % amplitude; 0.7 s ON, 1.3 s OFF, total of 30 seconds, 3 cycles(G Hendrickson et al., 2016) with Micro probe

while on ice. After sonication, the samples were centrifuged at 13000 x g for 10 minutes at 4 °C. The supernatants were used for analyses by SDS-PAGE- Western blot.

SDS-PAGE AND WESTERN BLOT

The lysates were prepared for SDS -PAGE by mixing in 2x Laemmli buffer (125 mM Tris-Cl (pH 6.8), 20 % glycerol, 4 % SDS and 3 % beta mercaptoethanol) and boiled for 5 minutes, and then loaded to freshly prepared denaturing Polyacrylamide gel prepared with the aid of Biorad mini protean casting system. Using Biorad mini protean running apparatus, the gels were run with at 80V for stacking and 120 V for resolving gels.

The gels were wet blotted (by Biorad Mini-Trans-Blot Electrophoretic Transfer Cell) on to nitrocellulose membrane (Amersham™ Protran) for 1.5 hours (0.75 mm gel thickness) at constant 100V. The membranes were blocked with the blocking buffer that contains 5 % skimmed milk (origin) in Phosphate Buffered Saline with 0.1 % Tween 20 (PBST) for 30 minutes at room temperature. The primary antibodies and their respective dilution in blocking buffer were: Anti YAP1 (Sigma Aldrich WH0010413M)-1/2000; anti-p53 (Sigma Aldrich- SAB5100001)-1/2000; Anti-GFP antibody (ab6556)-1/2000; anti G3BP1-1/2000 (abcam ab56574), anti-FUS-1/2000 (abcam ab23439); anti H3-1/4000 (Sigma Aldrich-H0164). Primary antibodies were incubated overnight at 4°C. Secondary antibodies used were goat anti-mouse IgG-HRP (sc-2005) and goat anti-rabbit IgG-HRP (sc-2004). The blots were developed with Western blot chemiluminescent substrate (Pierce ECL Thermo Scientific cat no. 32109).

IMMUNOPRECIPITATION

First, SDS concentration in the lysate was reduced to 0.05 % in order to prevent denaturation of the antibody: this was done by adding an equal volume of lysis buffer (for lysis of cells from 3 cm plate-400 ml was used) containing only the non-ionic detergent. The diluted lysates were added with 20 µl of Protein A Dynabeads (Invitrogen™ -10002D, 30 mg/ml). The beads were pre-equilibrated in the same lysis-buffer for 30 minutes at 4°C, then magnetized and resuspended in 20 ul. Preclearing of the lysate was done at 4°C for 30 minutes in tube rotator. The precleared lysate was then incubated with 1-2 ug of the Anti YAP1 (Sigma Aldrich WH0010413M) for 30 minutes in the cold. The antibody-lysate mixture was then incubated with 10 ul pre-equilibrated Protein A beads for another 30 minutes as before. After 30 minutes, magnetization was performed and the unbound supernatant fraction was recovered and transferred in a fresh tube, while the magnetic beads were washed quickly and gently with TBS. For GFP immunoprecipitation, 15 µl anti-GFP tagged magnetic beads (ChromoTek GFP-Trap®), washed with excess volume of lysis buffer and resuspended in 15 ul of the

same as for Protein A beads and was added to the diluted-precleared lysate and incubated for 30 minutes at 4°C. For protein analysis recovered beads from immunoprecipitation steps were resuspended in 40 µl of 2x Laemmli buffer was added and the samples were boiled at 95 °C for 5 minutes, or 70°C as specified.

EXTRACTION OF COMPLEXES WITH COOH BEADS

About 8×10^5 cells cultured on 3 cm tissue culture plate were fixed with the specified concentration of GA, FA or combination as explained in HTS section with the unfixed cells used as control. The carboxy conjugated magnetic beads used for this process were washed and preequilibrated with the TBS before the start of fixation. After fixation and quick wash with TBS, 600 µl of lysis buffer containing 50 mM Tris-Cl, pH 7.8, 100 mM NaCl, 1 % NP40, 2 mM EDTA was added along with 30 µl Carboxy conjugated Magnetic beads (Magnefy™, Bangs Laboratories Inc) and kept on ice for 5 minutes. Then, cells were scraped into fresh tubes and incubated again for 10 minutes and mixed by inverting up and down 3-4 times. The supernatant was separated using magnetic support and collected into fresh tubes. Then, the magnetic beads were resuspended in 600 µl of 2x Laemmli buffer and boiled for 5 mins. Equal volumes of supernatants and beads extract were loaded and analysed by SDS PAGE followed by Western blot.



REFERENCES

- An, H., Tan, J. T. and Shelkownikova, T. A. (2019) 'Stress granules regulate stress-induced paraspeckle assembly', *Journal of Cell Biology*, 218(12), pp. 4127–4140. doi: 10.1083/JCB.201904098.
- Banani, S. F. *et al.* (2017) 'Biomolecular condensates: Organizers of cellular biochemistry', *Nature Reviews Molecular Cell Biology*. Nature Publishing Group, 18(5), pp. 285–298. doi: 10.1038/nrm.2017.7.
- Bentley, E. P., Frey, B. B. and Deniz, A. A. (2019) 'Physical Chemistry of Cellular Liquid-Phase Separation', *Chemistry - A European Journal*, 25(22), pp. 5600–5610. doi: 10.1002/chem.201805093.
- Bergeron-Sandoval, L. P., Safaee, N. and Michnick, S. W. (2016) 'Mechanisms and Consequences of Macromolecular Phase Separation', *Cell*. Elsevier Inc., 165(5), pp. 1067–1079. doi: 10.1016/j.cell.2016.05.026.
- Bogen, S., Vani, K. and Sompuram, S. (2009) 'Molecular mechanisms of antigen retrieval: antigen retrieval reverses steric interference caused by formalin-induced cross-links', *Biotechnic & Histochemistry*, 84(5), pp. 207–215. doi: 10.3109/10520290903039078.
- Brangwynne, C. P. *et al.* (2009) 'Germline P granules are liquid droplets that localize by controlled dissolution/condensation', *Science*, 324(5935), pp. 1729–1732. doi: 10.1126/science.1172046.
- Brent W. Sutherland, Judy Toews, J. K. (2008) 'Utility of formaldehyde cross-linking and mass spectrometry in the study of protein–protein interactions', *Journal of mass spectrometry*, (April), pp. 699–715. doi: 10.1002/jms.1415.
- Cai, D. *et al.* (2019) 'Phase separation of YAP reorganizes genome topology for long-term YAP target gene expression', *Nature Cell Biology*. Springer US, 21(12), pp. 1578–1589. doi: 10.1038/s41556-019-0433-z.
- Cohan, M. C. and Pappu, R. V. (2020) 'Making the Case for Disordered Proteins and Biomolecular Condensates in Bacteria', *Trends in Biochemical Sciences*. Elsevier Ltd, 45(8), pp. 668–680. doi: 10.1016/j.tibs.2020.04.011.
- Colantoni, A. *et al.* (2020) 'Zooming in on protein–RNA interactions: a multilevel workflow to identify interaction partners', *Biochemical Society Transactions*, 48(4), pp. 1529–1543. doi: 10.1042/BST20191059.
- Cordes, E. H. and Jencks, W. P. (1962) 'On the Mechanism of Schiff Base Formation and Hydrolysis', *Journal of the American Chemical Society*, 84(5), pp. 832–837. doi: 10.1021/ja00864a031.
- Dasti, A. *et al.* (2019) 'RNA-centric approaches to study RNA-protein interactions in vitro and in silico',

Methods. Elsevier, (March), pp. 0–1. doi: 10.1016/j.ymeth.2019.09.011.

de Lorenzo, V., Sekowska, A. and Danchin, A. (2015) ‘Chemical reactivity drives spatiotemporal organisation of bacterial metabolism’, *FEMS Microbiology Reviews*, 39(1), pp. 96–119. doi: 10.1111/1574-6976.12089.

Deniz, A. A. (2020) ‘Networking and Dynamic Switches in Biological Condensates’, *Cell*. Elsevier Inc., 181(2), pp. 228–230. doi: 10.1016/j.cell.2020.03.056.

Dyson, H. J. (2016) ‘Making Sense of Intrinsically Disordered Proteins’, *Biophysical Journal*. Biophysical Society, 110(5), pp. 1013–1016. doi: 10.1016/j.bpj.2016.01.030.

Dyson, H. J. and Wright, P. E. (2005) ‘Intrinsically unstructured proteins and their functions’, *Nature Reviews Molecular Cell Biology*, 6(3), pp. 197–208. doi: 10.1038/nrm1589.

Feldman, M. (1973) ‘Reactions of nucleic acids and nucleoproteins with formaldehyde’, *Prog Nucleic Acid Res Mol Biol*, 13, pp. 1–49. doi: 10.1016/s0079-6603(08)60099-9.

G Hendrickson, D. *et al.* (2016) ‘Widespread RNA binding by chromatin-associated proteins’, *Genome Biology*. Genome Biology, 17(1), p. 28. doi: 10.1186/s13059-016-0878-3.

Gasior, K. *et al.* (2019) ‘Partial demixing of RNA-protein complexes leads to intradroplet patterning in phase-separated biological condensates’, *Physical Review E*, 99(1), pp. 1–24. doi: 10.1103/PhysRevE.99.012411.

Gemayel, R. *et al.* (2015) ‘Variable Glutamine-Rich Repeats Modulate Transcription Factor Activity’, *Molecular Cell*. The Authors, 59(4), pp. 615–627. doi: 10.1016/j.molcel.2015.07.003.

Guo, L. and Shorter, J. (2015) ‘It’s Raining Liquids: RNA Tunes Viscoelasticity and Dynamics of Membraneless Organelles’, *Molecular Cell*. Elsevier Inc., 60(2), pp. 189–192. doi: 10.1016/j.molcel.2015.10.006.

Hennig, S. *et al.* (2015) ‘Prion-like domains in RNA binding proteins are essential for building subnuclear paraspeckles’, *Journal of Cell Biology*, 210(4), pp. 529–539. doi: 10.1083/jcb.201504117.

Hentze, M. W. *et al.* (2018) ‘A brave new world of RNA-binding proteins’, *Nature Reviews Molecular Cell Biology*. Nature Publishing Group, 19(5), pp. 327–341. doi: 10.1038/nrm.2017.130.

Hockensmith, J. W. *et al.* (1986) ‘Laser cross-linking of nucleic acids to proteins. Methodology and first applications to the phage T4 DNA replication system’, *Journal of Biological Chemistry*, 261(8), pp. 3512–

3518.

Hoffman, E. A. *et al.* (2015) 'Formaldehyde crosslinking: A tool for the study of chromatin complexes', *Journal of Biological Chemistry*, 290(44), pp. 26404–26411. doi: 10.1074/jbc.R115.651679.

Holden, P. and Horton, W. (2009) 'Crude subcellular fractionation of cultured mammalian cell lines', *BMC Research Notes*, 2. doi: 10.1186/1756-0500-2-243.

Hopwood, D. (1969) 'Fixatives and fixation: a review', *The Histochemical Journal*, 1(4), pp. 323–360. doi: 10.1007/BF01003278.

<https://www.creativebiomart.net/resource/principle-protocol-crosslinking-and-immunoprecipitation-clip-388.htm> (no date) *Crosslinking and ImmunoPrecipitation (CLIP)*. Available at: <https://www.creativebiomart.net/resource/principle-protocol-crosslinking-and-immunoprecipitation-clip-388.htm>.

Huebinger, J. *et al.* (2018) 'Quantification of protein mobility and associated reshuffling of cytoplasm during chemical fixation', (November), pp. 1–11. doi: 10.1038/s41598-018-36112-w.

Jain, S. *et al.* (2016) 'ATPase-Modulated Stress Granules Contain a Diverse Proteome and Substructure', *Cell*. Elsevier Inc., 164(3), pp. 487–498. doi: 10.1016/j.cell.2015.12.038.

Jankowsky, E. and Harris, M. E. (2015) 'Specificity and nonspecificity in RNA-protein interactions', *Nature Reviews Molecular Cell Biology*. Nature Publishing Group, 16(9), pp. 533–544. doi: 10.1038/nrm4032.

Johnson, T. J. A. (1993) 'Glutaraldehyde Cross-Linking-Fast and Slow Modes', *BIOCATALYST DESIGN FOR STABILITY AND SPECIFICITY*.

Karnovsky M J (1974) 'A formaldehyde-glutaraldehyde fixative of high osmolality for use in electron microscopy', *J Cell Biol*, 3(18), p. 200.

Kast, J. and Klockenbusch, C. (2010) 'Optimization of formaldehyde cross-linking for protein interaction analysis of non-tagged integrin β 1', *Journal of Biomedicine and Biotechnology*, 2010. doi: 10.1155/2010/927585.

Kim, B. *et al.* (2020) 'Viral cross-linking and solid-phase purification enables discovery of ribonucleoprotein complexes on incoming RNA virus genomes', *bioRxiv*, p. 2020.04.08.032441. doi: 10.1101/2020.04.08.032441.

- Koulouras, G. *et al.* (2018) 'EasyFRAP-web: A web-based tool for the analysis of fluorescence recovery after photobleaching data', *Nucleic Acids Research*. Oxford University Press, 46(W1), pp. W467–W472. doi: 10.1093/nar/gky508.
- Kustatscher, G. *et al.* (2015) 'Chromatin enrichment for proteomics', 9(9), pp. 2090–2099. doi: 10.1038/nprot.2014.142.Chromatin.
- Lanier, K. A., Petrov, A. S. and Williams, L. D. (2017) 'The Central Symbiosis of Molecular Biology: Molecules in Mutualism', *Journal of Molecular Evolution*. Springer US, 85(1–2), pp. 8–13. doi: 10.1007/s00239-017-9804-x.
- Lee, F. C. Y. and Ule, J. (2018) 'Advances in CLIP Technologies for Studies of Protein-RNA Interactions', *Molecular Cell*. Elsevier Inc., 69(3), pp. 354–369. doi: 10.1016/j.molcel.2018.01.005.
- Li, P. *et al.* (2012) 'Phase transitions in the assembly of multivalent signalling proteins', *Nature*. Nature Publishing Group, 483(7389), pp. 336–340. doi: 10.1038/nature10879.
- Lin, Y. *et al.* (2015) 'Formation and Maturation of Phase-Separated Liquid Droplets by RNA-Binding Proteins', *Molecular Cell*. Elsevier Inc., 60(2), pp. 208–219. doi: 10.1016/j.molcel.2015.08.018.
- Matheny, T. *et al.* (2020) 'RNA partitioning into stress granules is based on the summation of multiple interactions', *bioRxiv*, p. 2020.04.15.043646. doi: 10.1101/2020.04.15.043646.
- McKenzie, A. T. (2019) *Glutaraldehyde: A review of its fixative effects on nucleic acids, proteins, lipids, and carbohydrates*, *OSF preprints*. doi: Web.
- Migneault, I. *et al.* (2004) 'Glutaraldehyde: behavior in aqueous solution, reaction with proteins, and application to enzyme crosslinking Isabelle', *Journal of Materials Chemistry A*, (37), pp. 790–802. doi: 10.1039/C6TA07211A.
- Mitrea, D. M. and Kriwacki, R. W. (2016) 'Phase separation in biology; Functional organization of a higher order Short linear motifs - The unexplored frontier of the eukaryotic proteome', *Cell Communication and Signaling*. Cell Communication and Signaling, 14(1), pp. 1–20. doi: 10.1186/s12964-015-0125-7.
- Modenez, I. A. *et al.* (2018) 'Influence of dlutaraldehyde cross-linking modes on the recyclability of immobilized lipase b from candida antarctica for transesterification of soy bean oil', *Molecules*, 23(9). doi: 10.3390/molecules23092230.

- Mohammad Lellahi, S. *et al.* (2018) ‘The long noncoding RNA NEAT1 and nuclear paraspeckles are up-regulated by the transcription factor HSF1 in the heat shock response’, *Journal of Biological Chemistry*, 293(49), pp. 18965–18976. doi: 10.1074/jbc.RA118.004473.
- Niranjanakumari, S. *et al.* (2002) ‘Reversible cross-linking combined with immunoprecipitation to study RNA-protein interactions in vivo’, *Methods*, 26(2), pp. 182–190. doi: 10.1016/S1046-2023(02)00021-X.
- Nott, T. J. *et al.* (2015) ‘Phase Transition of a Disordered Nuage Protein Generates Environmentally Responsive Membraneless Organelles’, *Molecular Cell*. The Authors, 57(5), pp. 936–947. doi: 10.1016/j.molcel.2015.01.013.
- Ouimet, C. M. *et al.* (2018) ‘Protein Cross-linking Capillary Electrophoresis at Increased Throughput for a Range of Protein-Protein Interactions’, 143(8), pp. 1805–1812. doi: 10.1039/C7AN02098H.Protein.
- Paavilainen, L. *et al.* (2010) ‘The impact of tissue fixatives on morphology and antibody-based protein profiling in tissues and cells’, *Journal of Histochemistry and Cytochemistry*, 58(3), pp. 237–246. doi: 10.1369/jhc.2009.954321.
- Patel, A. *et al.* (2015) ‘A Liquid-to-Solid Phase Transition of the ALS Protein FUS Accelerated by Disease Mutation’, *Cell*. Elsevier Inc., 162(5), pp. 1066–1077. doi: 10.1016/j.cell.2015.07.047.
- Ramanathan, M., Porter, D. F. and Khavari, P. A. (2019) ‘Methods to study RNA–protein interactions’, *Nature Methods*. Springer US, 16(3), pp. 225–234. doi: 10.1038/s41592-019-0330-1.
- Romero, P. *et al.* (1997) ‘Identifying disordered regions in proteins from amino acid sequence’, *Proceedings of International Conference on Neural Networks (ICNN’97)*, 1(June), pp. 1–6. doi: 10.1109/ICNN.1997.611643.
- Sabatini, D. D., Bensch, K. and Barnett, R. J. (1963) ‘Enzyme Cytochemistry and Electron Microscopy’, *Journal of the Royal Microscopical Society*, 81(3–4), pp. 173–177. doi: 10.1111/j.1365-2818.1963.tb02088.x.
- Schindelin, J. *et al.* (2012) ‘Fiji: An open-source platform for biological-image analysis’, *Nature Methods*, 9(7), pp. 676–682. doi: 10.1038/nmeth.2019.
- Schmiedeberg, L. *et al.* (2009) ‘A Temporal threshold for formaldehyde crosslinking and fixation’, *PLoS ONE*, 4(2). doi: 10.1371/journal.pone.0004636.
- Shin, Y. and Brangwynne, C. P. (2017) ‘Liquid phase condensation in cell physiology and disease’, *Science*,

357(6357), p. eaaf4382. doi: 10.1126/science.aaf4382.

Singh, G., Ricci, E. P. and Moore, M. J. (2014) 'RIPiT-Seq: A high-throughput approach for footprinting RNA: Protein complexes', *Methods*. Elsevier Inc., 65(3), pp. 320–332. doi: 10.1016/j.ymeth.2013.09.013.

Stancheva, I. *et al.* (1997) 'Chromatin structure and methylation of rat rRNA genes studied by formaldehyde fixation and psoralen cross-linking', *Nucleic Acids Research*, 25(9), pp. 1727–1735. doi: 10.1093/nar/25.9.1727.

Tauber, G. (2019) 'Principles and Properties of RNA Self-Assembly', pp. 1–27. Available at: https://scholar.colorado.edu/honr_theseshttps://scholar.colorado.edu/honr_theses/2028.

Tenenbaum, S. A. *et al.* (2002) 'Ribonomics: Identifying mRNA subsets in mRNP complexes using antibodies to RNA-binding proteins and genomic arrays', *Methods*, 26(2), pp. 191–198. doi: 10.1016/S1046-2023(02)00022-1.

Ule, J. *et al.* (2003) 'CLIP Identifies Nova-Regulated RNA Networks in the Brain', *Science*, 302(5648), pp. 1212 LP – 1215. doi: 10.1126/science.1090095.

Urdaneta, E. C. and Beckmann, B. M. (2019) 'Fast and unbiased purification of RNA-protein complexes after UV cross-linking'.

Vassar, P. S. *et al.* (1972) 'Physicochemical effects of aldehydes on the human erythrocyte', *Journal of Cell Biology*, 53(3), pp. 809–818. doi: 10.1083/jcb.53.3.809.

Weiss, M. (2014) *Crowding, diffusion, and biochemical reactions*. 1st edn, *International Review of Cell and Molecular Biology*. 1st edn. Elsevier Inc. doi: 10.1016/B978-0-12-800046-5.00011-4.

Whipple, E. B. and Ruta, M. (1973) 'Structure of Aqueous Glutaraldehyde', 39(12), pp. 1666–1668.

Wilson, E. B. (1899) 'THE STRUCTURE OF PROTOPLASM', *Science*, 10(237), pp. 33 LP – 45. doi: 10.1126/science.10.237.33.

Wojciak, J. M. *et al.* (2009) 'Structural basis for recruitment of CBP/p300 coactivators by STAT1 and STAT2 transactivation domains', *EMBO Journal*, 28(7), pp. 948–958. doi: 10.1038/emboj.2009.30.

Wurtz, J. D. and Lee, C. F. (2018) 'Chemical-Reaction-Controlled Phase Separated Drops: Formation, Size Selection, and Coarsening', *Physical Review Letters*. American Physical Society, 120(7), p. 78102. doi:

10.1103/PhysRevLett.120.078102.

Xiao, L. and Xiang, D. F. (2019) 'Chromatin-associated RNAs as facilitators of functional genomic interactions', *Physiology & behavior*, 20(9), pp. 503–519. doi: 10.1038/s41576-019-0135-1.

Yang, P. *et al.* (2020) 'G3BP1 Is a Tunable Switch that Triggers Phase Separation to Assemble Stress Granules', *Cell*, 181(2), pp. 325-345.e28. doi: 10.1016/j.cell.2020.03.046.

Zeng, F., Yang, W. and Huang, J. (2013) 'Determination of the lowest concentrations of aldehyde fixatives for completely fixing various cellular structures by real-time imaging and quantification'. doi: 10.1007/s00418-012-1058-5.



ACKNOWLEDGEMENTS

First of all, I express sincere gratitude to my Supervisor, Professor Claudio Schneider for his constant guidance and support throughout my PhD. His critical approach of science kept me curious throughout my research and let me learn a new perspective of science.

Then, I would like to thank my mentor's Dr Roberto Verardo (LNCIB) and Dr Enio Klaric (LNCIB) for their wonderful insights and teaching all these years. I also sincerely thank Dr Francesca De Este (DAME, Uniud) for her extreme patience in performing FRAP and giving valuable inputs in data analysis. I would like to thank Dr Edoardo Schneider for his help in performing High Throughput Imaging facility at ICGEB, Trieste.

I cannot express enough thanks to Professor Claudio Brancolini for being kind to accommodate me in his lab during the last period of my PhD. It would not either be complete without mentioning my thanks to his wonderful group-Dr Eros, Dr Terasa, Luca, Martina, Liliana, and Sowmeya

I am highly indebted to my parents and brothers for their constant motivation and support until this point of my life and letting me follow my dreams.

To my wonderful husband, Ayush Kumar Srivatsava, it would have not been possible for me to reach completion without your support and critical acknowledgements. A deep thanks to my extended family of in-laws, who is always proud of my hard work and achievements.

Next, I must thank my dear friends Yamanappa Hunashal, Arushi Vats and Vipin for their support and love.

Last but not least, I would not forget to thank my friends and relatives from India who constantly check me out for my well-being abroad.

And Thanks to Almighty for his Greatness!